HHS Public Access

Author manuscript

Nat Commun. Author manuscript; available in PMC 2015 August 18.

Published in final edited form as:

Nat Commun. ; 6: 6224. doi:10.1038/ncomms7224.

Dendritic cells induce Th2-mediated airway inflammatory responses to house dust mite via DNA-dependent protein kinase

Amarjit Mishra[1,7], **Alexandra L. Brown**[2,7], **Xianglan Yao**[1], **Shutong Yang**[2], **Sung-Jun Park**[2], **Chengyu Liu**[3], **Pradeep K. Dagur**[4], **J. Philip McCoy**[4], **Karen J. Keeran**[5], **Gayle Z. Nugent**[5], **Kenneth R. Jeffries**[5], **Xuan Qu**[6], **Zu-Xi Yu**[6], **Stewart J. Levine**[1,8], and **Jay H. Chung**[2,8]

[1]Laboratory of Asthma and Lung Inflammation, Division of Intramural Research, NHLBI, NIH.

[2]Laboratory of Obesity and Aging Research, Division of Intramural Research, NHLBI, NIH.

[3]Transgenic Core Facility, Division of Intramural Research, NHLBI, NIH.

[4]Flow Cytometry Core Facility, Division of Intramural Research, NHLBI, NIH.

[5]Animal Surgery and Resources Core Facility, Division of Intramural Research, NHLBI, NIH.

[6]Pathology Core Facility, Division of Intramural Research, NHLBI, NIH.

Abstract

DNA-dependent protein kinase (DNA-PK) mediates double stranded DNA break repair, V(D)J recombination, and immunoglobulin class switch recombination, as well as innate immune and pro-inflammatory responses. However, there is limited information regarding the role of DNA-PK in adaptive immunity mediated by dendritic cells (DCs), which are the primary antigen-presenting cells in allergic asthma. Here we show that house dust mite induces DNA-PK phosphorylation, which is a marker of DNA-PK activation, in DCs via the generation of intracellular reactive oxygen species. We also demonstrate that pharmacological inhibition of DNA-PK, as well as the specific deletion of DNA-PK in DCs, attenuates the induction of allergic sensitization and Th2 immunity via a mechanism that involves the impaired presentation of mite antigens. Furthermore, pharmacological inhibition of DNA-PK following antigen priming similarly reduces the manifestations of mite-induced airway disease. Collectively, these findings suggest that DNA-PK may be a potential target for treatment of allergic asthma.

Correspondence should be addressed to S.J.L. (levines@nhlbi.nih.gov) or J.H.C. (chungj@nhlbi.nih.gov).
[7]These authors contributed equally to this work.
[8]These authors jointly supervised this work.

The authors declare no competing financial interests.

Author Contributions

AM and ALB together with XY, SY, SJP, PKD, KJK, GZN, KRJ and XQ performed the experiments; ALB, SY, CL and JHC generated the *DNA-PKcs*$^{fl/fl}$ mice; AM, ALB, PKD, JPM, ZXY, SJL and JHC analyzed the data; AM, ALB, PKD, JPM, SJL and JHC wrote the manuscript.

Introduction

DNA-dependent protein kinase (DNA-PK) is a key enzyme involved in the recognition and repair of double stranded DNA breaks (DSB) by a process termed nonhomologous end-joining (NHEJ) whereby DNA ends are directly ligated[1, 2, 3, 4]. This represents an important mechanism of cellular repair in response to DSB induced by ionizing radiation, as well as reactive oxygen species, that prevents chromosomal translocations and genetic instability that can lead to carcinogenesis or cellular death[2, 5]. DNA-PK is comprised of a regulatory heterodimer of Ku proteins (Ku70 and Ku80) and a 465 kDa catalytic subunit, DNA-PKcs, which is a member of the phosphatidylinositol 3-kinase-related kinase (PIKK) family and functions as a serine/threonine kinase.

DNA-PK also participates in additional processes that involve DSB repair, such as V(D)J recombination and class switch recombination[2, 6]. Mice with the *scid* mutation affecting the *Prkdc* gene that encodes DNA-PKcs are unable to generate functional immunoglobulin and T cell receptors and are deficient in mature B and T lymphocytes[7, 8, 9, 10]. The *scid* missense mutation results in a premature stop codon that leads to diminished expression of the DNA-PKcs protein and specifically impairs the differentiation of stem cells into mature lymphocytes, whereas myeloid differentiation is not affected[9, 11, 12]. Similarly, mice with a targeted disruption of the *Prkdc* gene, which encodes DNA-PKcs, have a phenotype of severe combined immunodeficiency (SCID) and radiosensitivity[13].

Although its canonical function is to mediate DSB repair by NHEJ, DNA-PK has also been shown to regulate innate immune responses and pro-inflammatory signaling pathways[2, 4]. For example, DNA-PK modulates host defense against viral infection by acting as a pattern recognition receptor that binds cytoplasmic DNA[14]. This activates an innate immune response mediated by type I interferons via a pathway involving IRF-3 (interferon regulatory factor 3), TBK1 (TANK-binding kinase 1) and STING (stimulator of interferon genes). Interestingly, vaccinia virus (VACV) has evolved a strategy to evade this mechanism[15]. The VACV C16 protein directly binds the Ku heterodimer, thereby blocking DNA-PK binding to DNA, which inhibits DNA sensing and innate immunity to DNA viruses. The mechanism of killing of $CD4^+$ T cells during human immunodeficiency virus-1 (HIV-1) infection has also recently been shown to involve DNA-PK activation[16]. Integration of the HIV-1 genome into the host chromosome induces a double stranded DNA damage response that activates DNA-PK and phosphorylates p53 and histone H2AX, with resultant death of $CD4^+$ cells. Interestingly, HIV-1-mediated $CD4^+$ cell death could be inhibited by pharmacological inhibitors of DNA-PK. Infection with *Listeria monocytogenes* also causes DNA strand breaks that induce the phosphorylation and activation of DNA-PK, H2AX and CDC25A. This activates a DNA damage/replication checkpoint that delays cell cycle progression and thereby facilitates propagation of this intracellular pathogen[17]. DNA-PK also participates in an endosomal signaling pathway that induces a pro-inflammatory response in natural killer cells by phosphorylating Akt on Ser^{473} [18]. The DNA-PK-mediated phosphorylation of p50 NF-κB is similarly required for tumor necrosis factor-induced VCAM-1 expression[19]. Lastly, DNA-PK mediates free fatty acid-induced lipid accumulation in hepatocytes, which may contribute to the pathogenesis of nonalcoholic steatohepatitis[20].

Since DNA-PK can regulate innate immunity and pro-inflammatory signaling pathways, we hypothesized that it might also modulate adaptive Th2-mediated immune responses to house dust mite (HDM) antigen. We also hypothesized that if DNA-PK were involved in the pathogenesis of HDM-induced asthma, then pharmacological inhibitors of DNA-PK kinase activity might be utilized as a novel treatment approach. We focused on HDM because it is a clinically important aeroallergen that is a potent inducer of Th2-mediated immune responses and a common cause of allergic asthma worldwide. To investigate the role of DNA-PK in HDM-induced asthma, here we utilize genetic and pharmacological models, including the development of a CD11c-specific DNA-PKcs knockout mouse. We show that HDM activates DNA-PK in dendritic cells (DCs) via a ROS-dependent pathway. Furthermore, we show that DNA-PK is required for both effective antigen presentation by DCs, as well as the induction of HDM-induced Th2-mediated airway inflammation. This demonstrates a previously unidentified link between the role of DNA-PK in DCs and the induction of allergic sensitization and Th2 immunity in HDM-induced asthma. Furthermore, it identifies DNA-PK as a novel therapeutic target for the development of new treatments for asthmatic patients.

Results

House Dust Mite induces DNA-PK Phosphorylation in Dendritic Cells

First, we considered whether HDM could induce the generation of intracellular reactive oxygen species (ROS) by human monocyte-derived dendritic cells (moDCs) as a mechanism by which DNA-PK phosphorylation and activation are initiated. Stimulation of human moDCs with HDM induced the production of intracellular ROS, which could be inhibited by the anti-oxidant, NAC (*N*-acetylcysteine), the NADPH oxidase/flavoprotein inhibitor, DPI (diphenyleneiodonium chloride), and the DNA-PK inhibitor, NU7441 (Figure 1A)[21]. We then assessed whether human moDCs express DNA-PK and whether DNA-PK can be activated in response to HDM stimulation. Western blots of human moDC proteins demonstrated that DNA-PKcs is expressed under basal conditions and is activated in response to HDM stimulation, as evidenced by auto-phosphorylation on Ser^{2056}, which is a marker of DNA-PK activity (Figure 1B)[22]. DNA-PK activity peaks at 3 and 6 hours and markedly diminishes by 24 hours. HDM-induced DNA-PK phosphorylation at Ser^{2056} at 6 hours was inhibited by treatment with NU7441, as well as NAC and DPI[21]. HDM stimulation also induced Akt phosphorylation on Ser^{473} and Thr^{308} that was maximal at 6 and 24 hours. Levels of p-Akt (Ser^{473}) and p-Akt (Thr^{308}) were similarly reduced by NU7441, NAC and DPI. Collectively, these results demonstrate that HDM stimulates intracellular ROS generation by human moDCs and that ROS are required for the HDM-induced phosphorylation of DNA-PK, as well as Akt, which is downstream of DNA-PK signaling and has been reported to be a regulator of DC function[23].

Experiments were next performed with bone marrow-derived dendritic cells (BMDCs) from $Prkdc^{scid}$ mice that have a spontaneous mutation in the *Prkdc* gene. HDM-challenged BMDCs from wild type (WT), but not $Prkdc^{scid}$ mice, had increases in intracellular ROS generation (Figure 1C). Thus, in addition to being activated by ROS, DNA-PK is required for HDM-induced ROS production by BMDCs. Next, BMDCs from $Prkdc^{scid}$ mice were

used to investigate the role of DNA-PK in antigen-specific T cell proliferation and Th2 cytokine production. Co-culture experiments of splenic $CD4^+$ T cells from mice expressing the MHCII-restricted DO11.10 T-cell receptor that recognizes the OVA 323–339 peptide showed that BMDCs from *Prkdc*^{scid} mice have a reduced ability to induce both T cell proliferation and Th2 cytokine production as compared to BMDCs from WT mice following *ex vivo* stimulation with the OVA 323–339 peptide (Figures 1D–G)[24]. Similarly, BMDCs from *Prkdc*^{scid} mice had an impaired ability to induce Th2 cytokine production following *ex vivo* stimulation with full-length ovalbumin when co-cultured with splenic T cells from OVA-sensitized mice. Collectively, this shows that DNA-PK-deficient dendritic cells have a primary defect in antigen presentation to T cells and are unable to mediate the antigen-specific production of Th2 effector cytokines. Lastly, we show that both murine BMDCs and human moDCs express the co-stimulatory molecules, CD40, CD80 and CD86 (Figure 1 H). Furthermore, HDM stimulation increased expression of CD86 by murine BMDCs and CD40 by human moDCs.

Dendritic Cells from *Prkdc*^{scid} mice Mediate Reduced Th2 Inflammation

Adoptive transfer experiments using HDM-pulsed $CD11c^+$ BMDCs from WT and *Prkdc*^{scid} mice were next utilized to define the role of dendritic cell DNA-PK in inducing Th2-mediated airway inflammatory responses to HDM (Figure 2A). Bronchoalveolar lavage fluid (BALF) from HDM-challenged WT mice that had received the adoptive transfer of HDM-pulsed BMDCs from WT mice (WT BMDCs) had significant increases in inflammatory cells as compared to HDM-challenged WT mice that had received the adoptive transfer of HDM-pulsed BMDCs from *Prkdc*^{scid} mice (*scid* BMDCs) (Figure 2B). Similarly, HDM-challenged recipients of adoptively transferred WT BMDCs that had been pulsed with HDM had an increase in peri-bronchial inflammatory cell infiltrates on lung histology as compared to recipients of HDM-pulsed *scid* BMDCs (Figure 2C). HDM re-stimulation of cultures of mediastinal lymph node (MLN) cells from HDM-challenged mice showed a significant reduction in the production of the Th2 effector cytokines, IL-4, IL-5 and IL-13, in recipients of *scid* BMDCs as compared to WT BMDCs (Figure 2D). BALF levels of C-C chemokines that recruit eosinophils and T cells to the lung, were also significantly reduced in recipients of *scid* BMDCs as compared to WT BMDCs (Figure 2E–H). These include CCL24 (eotaxin-2), which interacts with CCR3 to recruit eosinophils, CCL17 (TARC) and CCL22 (MDC), which interacts with CCR4 on Th2 cells, and CCL5 (RANTES), which interacts with CCR5 that is highly expressed on T cells in the lung[25, 26]. Lastly, serum levels of HDM-specific IgE were significantly reduced in recipients of *scid* BMDCs as compared to WT BMDCs, thereby demonstrating the reduced ability of *scid* BMDCs to induce allergic sensitization (Figure 2I). Collectively, these results demonstrate that DNA-PK-deficient dendritic cells are defective in the initiation of HDM-mediated allergic sensitization and Th2-mediated airway inflammatory responses.

DNA-PK Inhibition Attenuates Dendritic Cell-mediated Th2 Inflammation

Experiments were next conducted to assess whether $CD11c^+$ BMDCs that had been treated *ex vivo* with the DNA-PK inhibitor, NU7441, have a reduced ability to induce Th2-mediated allergic airway inflammation in response to HDM (Figure 3A). Recipients of adoptively transferred HDM-pulsed WT DCs that had been treated with NU7441 had significant

reductions in the number of BALF inflammatory cells as compared to recipients of HDM-pulsed WT DCs that had been treated with medium alone (Figure 3B). Consistent with this, lung histology showed a reduction in peri-bronchial inflammatory cell infiltrates in recipients of HDM-pulsed WT DCs that had been treated with NU7441, which was associated with a reduction in mucous cell metaplasia (Figures 3C and 3D). HDM re-stimulation of *ex vivo* cultures of MLN cells from recipients of NU7441-treated HDM-pulsed BMDCs had a reduced ability to produce the Th2 cytokines, IL-4, IL-5, and IL-13 as compared to recipients of HDM-pulsed WT DCs treated with medium alone (Figure 3E). BALF levels of the anti-inflammatory cytokine, IL-10, were significantly higher in recipients of NU7441-treated HDM-pulsed WT DCs (Figure 3F), whereas BALF levels of chemokines (CCL5, CCL17, CCL22 and CCL24) were significantly reduced (Figure 3G). Lastly, serum levels of HDM-specific IgE were significantly reduced in recipients of NU7441-treated HDM-pulsed WT DCs, indicating impaired allergic sensitization (Figure 3H). These results demonstrate that NU7441-mediated pharmacological inhibition of DNA-PK in BMDCs impairs their ability to initiate HDM-mediated allergic sensitization and Th2-mediated airway inflammatory responses.

If Akt is downstream of DNA-PK signaling in DCs, then treatment of adoptively transferred DCs with GDC0068, a pharmacological inhibitor of Akt kinase activity, would be predicted to have the same effect as treatment of BMDCs with NU7441 prior to adoptive transfer. Consistent with this concept, WT recipient mice that received the adoptive transfer of HDM-pulsed $CD11c^+$ BMDCs that had been treated *ex vivo* with GDC0068 demonstrated significant reductions in the BALF inflammatory cells (Figure 3I) and mucous cell metaplasia (Figure 3J). In addition, recipients of GDC0068-treated HDM-pulsed WT DCs had reductions in Th2 cytokine production by MLN cells that had been re-stimulated *ex vivo* with HDM (Figure 3K), as well as an increase in BALF IL-10 levels, as compared to recipients of HDM-pulsed WT DCs that had not been treated with GDC0068 (Figure 3L). Collectively, these results are consistent with the conclusion that Akt is downstream of DNA-PK signaling in DCs.

CD11c-specific *DNA-PKcs* Knockout Mice Have Impaired Th2 Inflammation

Next, we considered whether the specific deletion of DNA-PKcs in $CD11c^+$ dendritic cells would similarly impair the induction of allergic sensitization and Th2 immune response to HDM. *DNA-PKcs*$^{fl/fl}$ mice were created with loxP sites flanking exons 82 and 83 of the *Prkdc* gene (Figure 4A). Exons 82 and 83, along with exon 81, comprise the kinase catalytic domain of DNA-PKcs and human cells with deletions of these exons have both undetectable kinase activity and DNA-PKcs protein expression[27]. The insertion of the LoxP sites in the floxed allele of the *Prkdc* gene was confirmed by Southern blotting of genomic DNA from *DNA-PKcs*$^{fl/+}$ mice (Figure 4B). *DNA-PKcs*$^{fl/fl}$ mice were bred with *CD11c*-Cre mice to generate homozygous *DNA-PKcs*$^{fl/fl;}$ *CD11c*-Cre mice in which DNA-PKcs expression is specifically deleted in $CD11c^+$ DCs, but not in other cells, such as airway epithelial cells (Figure 4C). As shown in Figure 4D, *DNA-PKcs* mRNA levels were 15.5 fold higher in splenic DCs isolated from *DNA-PKcs*$^{fl/fl}$ as compared to those from *DNA-PKcs*$^{fl/fl;}$ *Cd11c*-Cre mice. The deletion of exons 82 and 83 of the *Prkdc* gene was further confirmed by sequencing of genomic DNA from $CD11c^+$ splenic DCs isolated from DNA-PKcs $^{fl/fl}$;

CD11c-Cre mice (Supplementary Figure 1). *DNA-PKcs*$^{fl/fl;}$ *CD11c*-Cre mice then received multiple intranasal HDM challenges to assess the effect of the CD11c-specific deletion of DNA-PKcs on HDM-induced airway inflammation and Th2 responses (Figure 5A). As shown in Figure 5B, the number of BALF inflammatory cells recovered from HDM-challenged *DNA-PKcs*$^{fl/fl;}$ *Cd11c*-Cre mice were significantly reduced as compared to those from HDM-challenged *DNA-PKcs*$^{fl/fl}$ mice. Similarly, lung histopathology showed a reduction in the extent of peri-bronchial inflammatory cell infiltrates in HDM-challenged *DNA-PKcs*$^{fl/fl;}$ *Cd11c*-Cre mice as compared to HDM-challenged *DNA-PKcs*$^{fl/fl}$ mice (Figure 5C). Mucous cell metaplasia was also significantly reduced in HDM-challenged *DNA-PKcs*$^{fl/fl;}$ *Cd11c*-Cre mice as compared to HDM-challenged *DNA-PKcs*$^{fl/fl}$ mice (Figures 5C and 5D). HDM re-stimulation of MLNs from *DNA-PKcs*$^{fl/fl;}$ *Cd11c*-Cre mice showed significant reductions in the Th2 cytokines, IL-5 and IL-13, whereas the reduction in IL-4 production was not statistically significant (Figure 5E). There was also no change in IFN-γ production by MLN cells following HDM re-stimulation. BALF levels of C-C chemokines, CCL17, CCL22, and CCL24, were also significantly reduced in HDM-challenged *DNA-PKcs*$^{fl/fl;}$ *Cd11c*-Cre mice as compared to HDM-challenged *DNA-PKcs*$^{fl/fl}$ mice, whereas there was no difference in levels of CCL5 (Figure 5F). Lastly, there was a significant reduction in serum levels of HDM-specific IgE in HDM-challenged *DNA-PKcs*$^{fl/fl;}$ *Cd11c*-Cre mice (Figure 5G). Collectively, these results demonstrate that *DNA-PKcs*$^{fl/fl;}$ *Cd11c*-Cre mice have an impaired ability to induce both allergic sensitization to HDM and Th2-mediated airway inflammatory responses.

Experiments were next conducted to assess the mechanisms by which DNA-PK-deficient CD11c^{+} DCs have a reduced capability to induce allergic sensitization and Th2 immunity to HDM. First, we assessed whether the percentage of T and B cells in naïve *DNA-PKcs*$^{fl/fl}$ and *DNA-PKcs*$^{fl/fl;}$ *Cd11c*-Cre mice were reduced as compared to the wild type (WT) parental strain of C57BL/6 mice, which could be indicative of a defect in V(D)J recombination with resultant altered lymphocyte development. As shown in Figure 6A and 6B, the percentage of CD3^{+} T cells and CD19^{+} B cells were not significantly different in the lungs and spleens of naïve WT, *DNA-PKcs*$^{fl/fl}$, and *DNA-PKcs*$^{fl/fl;}$ *Cd11c*-Cre mice, except for an increase in the percentage of splenic CD19^{+} B cells in *DNA-PKcs*$^{fl/fl;}$ *Cd11c*-Cre mice as compared to WT mice. This finding suggests that lymphocyte development was not significantly impaired in *DNA-PKcs*$^{fl/fl}$ and *DNA-PKcs*$^{fl/fl;}$ *Cd11c*-Cre mice. Second, we found that cell surface expression of the co-stimulatory molecule, CD80, was significantly reduced on CD11c^{+} DCs in the lungs (Figure 6C) and MLNs (Figure 6D) of HDM-challenged *DNA-PKcs*$^{fl/fl;}$ *Cd11c*-Cre mice as compared to HDM-challenged *DNA-PKcs*$^{fl/fl}$ mice. Although there were statistically significant differences in the expression of OX-40L, CD40 and CD86 by CD11c^{+} DCs in the lung and MLNs, these differences appeared modest as compared to the reduction in cell surface expression of CD80. In addition, as compared to the murine BMDCs and human moDCs that were utilized for the experiments in Figure 1H, CD11c^{+} DCs from the lungs and MLNs of *DNA-PKcs*$^{fl/fl}$ and *DNA-PKcs*$^{fl/fl;}$ *Cd11c*-Cre mice had a different pattern of expression of CD40, CD80 and CD86, as well as lower cell surface levels of these co-stimulatory molecules.

Next, we focused on CD11b$^+$ DCs, as these have been shown to be the primary DC subset that mediates antigen presentation and Th2 immunity[28, 29, 30]. We show that the percentage of CD11c$^+$ DCs that express CD11b were modestly reduced in the lungs (Figure 6E), but not the MLNs (Figure 6F) of *DNA-PKcs$^{fl/fl;}$ Cd11c*-Cre mice as compared to *DNA-PKcs$^{fl/fl}$* mice. Next, to assess the functional significance of the reduction in numbers of CD11b$^+$ DCs, AF647-labeled HDM was administered to the lungs of *DNA-PKcs$^{fl/fl;}$ Cd11c*-Cre and *DNA-PKcs$^{fl/fl}$* mice. As shown in Figure 6G and 6H, there was no difference in either uptake of HDM antigen in the lung or subsequent migration to MLNs by CD11c$^+$/MHCII$^+$/CD11b$^+$ DCs from *DNA-PKcs$^{fl/fl;}$ Cd11c*-Cre mice as compared to *DNA-PKcs$^{fl/fl}$* mice. Lastly, since DNA-PK has been reported to modulate the expression of toll-like receptors (TLR) in RAW264.7 macrophages by interacting with the autoimmune regulator, Aire, we assessed whether TLR expression by lung CD11b$^+$ DCs was modified in *DNA-PKcs$^{fl/fl;}$ Cd11c*-Cre mice as a possible mechanism by which T cell priming might be impaired[31]. As shown in Figure 6I and 6J, there was no difference in the percentage of lung CD11b$^+$ DCs that expressed TLR4 or TLR5, or the mean fluorescence intensity (MFI) of TLR4 and TLR5 expression by lung CD11b$^+$ DCs, in *DNA-PKcs$^{fl/fl}$* as compared to *DNA-PKcs$^{fl/fl;}$ Cd11c*-Cre mice. Thus, modified expression of TLR4 or TLR5 by lung CD11b$^+$ DCs does not appear to mediate impaired T cell priming to HDM in *DNA-PKcs$^{fl/fl;}$ Cd11c*-Cre mice. This is consistent with prior reports which found that expression of TLR4 by structural cells, such as airway epithelial cells, but not hematopoietic cells, such as DCs, mediates priming of Th2 cells to HDM through the airway, whereas both hematopoietic and structural cells are required for maximal TLR5-mediated allergic sensitization[32, 33].

We then assessed whether production of the anti-inflammatory cytokine, IL-10 was modified in *DNA-PKcs$^{fl/fl}$; Cd11c*-Cre mice as a mechanism by which HDM-associated inflammatory responses are decreased. As shown in Figure 6K, IL-10 was higher in BALF from HDM-challenged *DNA-PKcs$^{fl/fl;}$ Cd11c*-Cre mice as compared to HDM-challenged *DNA-PKcs$^{fl/fl}$* mice. Furthermore, BMDCs from *DNA-PKcs$^{fl/fl}$; Cd11c*-Cre mice secreted larger amounts of IL-10 in response to HDM stimulation as compared to those from *DNA-PKcs$^{fl/fl}$* mice (Figure 6L). Lastly, IL-10 secretion by HDM-stimulated BMDCs from *DNA-PKcs$^{fl/fl}$* mice was increased in response to GDC0068 and MK2206, pharmacological inhibitors of Akt, which is downstream of DNA-PK signaling (Figure 6M). Collectively, these results suggest that HDM-induced IL-10 production by DCs is suppressed via a DNA-PKcs/Akt pathway. We also assessed whether the number of CD3$^+$/CD4$^+$/CD25$^+$/Foxp3$^+$ regulatory T cells (Tregs) was modified in DNA-PKcs$^{fl/fl}$; CD11c-Cre mice. However, we found that there was no difference in the percentage of Tregs in MLNs of HDM-challenged *DNA-PKcs$^{fl/fl}$; Cd11c*-Cre mice as compared to *DNA-PKcs$^{fl/fl}$* mice (Figure 6N).

DNA-PK-deficient CD11b$^+$ DCs have Impaired Antigen Presentation

Since uptake of HDM antigen in the lung and trafficking to MLNs by CD11b$^+$ DCs from *DNA-PKcs$^{fl/fl}$; Cd11c*-Cre mice were not reduced, we next assessed whether CD11b$^+$ DCs from *DNA-PKcs$^{fl/fl}$; Cd11c*-Cre mice have an impairment in antigen presentation that limits their ability to induce allergic sensitization and Th2-mediated airway inflammation. CD11b$^+$ DCs were isolated from MLNs of *DNA-PKcs$^{fl/fl}$* and *DNA-PKcs$^{fl/fl}$; Cd11c*-Cre mice that had been challenged with HDM or saline and adoptively transferred to WT mice that

subsequently received intranasal HDM challenges to induce airway inflammation (Figure 7A). As shown in Figure 7B, the number alveolar macrophages, eosinophils, neutrophils and lymphocytes were significantly reduced in BALF from recipients of $CD11b^+$ DCs from *DNA-PKcs*$^{fl/fl}$*; Cd11c*-Cre donor mice as compared to *DNA-PKcs*$^{fl/fl}$ donor mice. Similarly, lung histology showed a reduction in peri-bronchial inflammatory cell infiltrates and mucous cell metaplasia in recipients of $CD11b^+$ DCs from *DNA-PKcs*$^{fl/fl}$*; Cd11c*-Cre donor mice as compared to *DNA-PKcs*$^{fl/fl}$ donor mice (Figures 7C and 7D). Serum levels of HDM-specific IgE were significantly reduced in recipients of $CD11b^+$ DCs from *DNA-PKcs*$^{fl/fl}$*; Cd11c*-Cre donor mice, while *ex vivo* cultures of MLNs that had been re-stimulated with HDM showed an impaired ability to produce IL-5 and IL-13 (Figures 7E and 7F). Collectively, these experiments demonstrate that $CD11b^+$ DCs from *DNA-PKcs*$^{fl/fl}$*; Cd11c*-Cre mice have an impairment in antigen presentation and the subsequent induction of allergic sensitization and Th2 immunity to HDM.

Pharmacological Inhibition of DNA-PK Suppresses HDM-induced Airway Disease

Lastly, we assessed whether pharmacologic inhibition of DNA-PK by consumption of chow containing NU7441 could attenuate HDM-induced airway disease in WT mice, which could provide evidence to support the concept of utilizing DNA-PK inhibitors for the treatment of asthmatic patients (Figure 8A). As shown in Figure 8B, mice that consumed chow containing 0.6% or 0.9% NU7441 had similar significant decreases in the number of BALF inflammatory cells. Lung histopathology similarly revealed that mice fed NU7441 had reductions in peri-bronchial inflammatory cell infiltrates (Figure 8C). In addition to the reductions in airway inflammation, NU7441 also attenuated HDM-mediated increases in mucous cell metaplasia (Figure 8D) and airway hyperresponsiveness (AHR) (Figure 8E). The reductions in airway inflammation and AHR were similar in mice that received chow containing either 0.6% or 0.9% NU7441.

Additional experiments were performed to characterize further the effects of NU7441 on indices of airway inflammation. As shown in Figure 9A, HDM re-stimulation of *ex vivo* MLN cultures from mice that had been fed chow containing NU7441 showed significant reductions in the production of the Th2 cytokines, IL-5 and IL-13, with or without *ex vivo* treatment with NU7441. Similarly, the number of BALF $CD4^+$ T cells were reduced in HDM-challenged mice that were fed chow containing NU7441, as were the number of IL-5^+ $CD4^+$ T cells, whereas the number of IL-13^+ $CD4^+$ T cells appeared to be decreased, but did not reach statistical significance (Figure 9B). The number of IL-17^+ $CD4^+$ T cells, however, was not reduced (Figure 9B). Mice that received NU7441 also had an increase in BALF IL-10 levels (Figure 9C) and a reduction in BALF CCL24 (Figure 9D). NU7441 also attenuated allergic sensitization as indicated by reduced plasma levels of HDM-specific IgE (Figure 9E). Collectively, these findings demonstrate that oral administration of a pharmacological DNA-PK inhibitor can attenuate allergen sensitization and Th2-mediated airway inflammation, as well as other cardinal manifestations of experimental HDM-induced asthma, including mucous cell metaplasia and AHR.

Lastly, experiments were performed to assess the effect of treatment with NU7441 after T cell priming had already occurred. As shown in Figure 10A, HDM-sensitized WT mice that

consumed chow containing 0.9% NU7441 concurrent with intranasal HDM challenges, but after allergic sensitization had already occurred, demonstrated a significant reduction in the number of BALF inflammatory cells (Figure 10 B and C), as well as in the extent of peri-bronchial inflammation on lung histology (Figure 10D). NU7441 (0.9%) treatment was also associated with reductions in serum levels of HDM-specific IgE (Figure 10E), mucous cell metaplasia (Figures 10D and 10F) and AHR (Figure 10G), whereas BALF IL-10 levels were significantly increased (Figure 10H). This demonstrates that oral administration of a pharmacological DNA-PK inhibitor only during the challenge phase can similarly attenuate the manifestations of HDM-induced asthma.

Discussion

DCs are the primary antigen presenting cells in the lung that induce allergic sensitization and Th2 adaptive immune responses to inhaled allergens, such as HDM, which is a common aeroallergen that causes asthma[34, 35]. DCs that reside in the airway take up antigens for processing in the context of MHCII, followed by migration to MLNs where they facilitate Th2 cell differentiation and production of key effector cytokines, such as IL-5 and IL-13. Consistent with this, transgenic mice that have been depleted of $CD11c^+$ DCs are not capable of mounting Th2 responses to HDM or HDM-induced pulmonary eosinophilia and lymphocytosis, whereas the adoptive transfer of $CD11c^+/MHCII^+$ cells is sufficient to induce Th2 immunity and pulmonary eosinophilia and lymphocytosis[35]. Limited and conflicting data, however, exists regarding the role of DNA-PK in DC function[36, 37, 38]. Prior studies using splenic $CD11c^+$ DCs and bone marrow-derived DCs (BMDCs) from *DNA-PKcs*$^{-/-}$ mice have found that DNA-PK was not required for production of IFN-α and IL-12 in response to oligodeoxynucleotides that contained unmethylated CpG motifs (CpG-ODN), which instead signaled via TLR9 and MyD88[36, 37]. A recent publication, however, has shown that BMDCs from *DNA-PKcs*$^{-/-}$ mice had reduced CpG-ODN-mediated production of IL-6 and IL-12[38]. Furthermore, CpG-ODN was shown to bind DNA-PKcs and induce its association with TRAF6.

Here, we investigated whether DNA-PK participates in DC-mediated induction of allergic sensitization to HDM and Th2-mediated airway inflammation. First, we show that DNA-PK is phosphorylated and activated in DCs in response to HDM stimulation by a mechanism that is dependent upon the generation of intracellular ROS. This is consistent with prior reports demonstrating that factors which activate DNA-PK are not restricted to DSB, but also include ROS and hypoxia[39, 40, 41]. We also show that the DNA-PK inhibitor, NU7441, as well as ROS inhibitors, NAC and DPI, attenuate HDM-mediated phosphorylation of Akt on Ser^{473} and Thr^{308}. This is consistent with the ability of DNA-PK to function as an upstream kinase that associates with and phosphorylates Akt on Ser^{473}, especially in the setting of DSB[42, 43]. This is also highly relevant to the induction of HDM-mediated allergic immune responses, as Akt signaling has been reported to regulate the activation and antigen presenting capability of DCs[23].

We also showed that HDM-stimulated BMDCs from *Prkdc*^{scid} mice were defective in ROS generation. DCs endogenously generate ROS during antigen presentation and ROS functions as a second messenger for MHCII-restricted antigen presentation with resultant activation of

CD4$^+$ Th2 cells to produce effector cytokines[44, 45, 46, 47, 48]. Therefore, we hypothesized that in the absence of DNA-PK, DCs might have an impaired ability to induce Th2-mediated adaptive immune responses to HDM. Here, we utilized several experimental models to demonstrate a key role for DNA-PK in the induction of allergic sensitization and Th2 effector cytokine production by dendritic cells in response to HDM. First, we showed that the adoptive transfer of HDM-pulsed CD11c$^+$ BMDCs from *Prkdc^{scid}* mice or wild type CD11c$^+$ BMDCs that had been treated with the DNA-PK inhibitor, NU7441, had an impaired ability to induce allergic sensitization, as indicated by a decrease in serum levels of HDM-specific IgE, as well as a reduction in production of Th2 effector cytokines, C-C chemokines and HDM-mediated airway inflammation. Next, a CD11c-conditional DNA-PKcs-deficient mouse was created to characterize further the role of DNA-PK expression by DCs in allergic sensitization. Similar to the adoptive transfer experiments, HDM-challenged *DNA-PKcs$^{fl/fl}$;* CD11c-Cre mice displayed a phenotype of impaired allergic sensitization and attenuated induction of Th2 immune responses to HDM that were associated with reductions in C-C chemokine production, airway inflammation and mucous cell metaplasia. Furthermore, CD11c$^+$ DCs in the lungs and MLNs from HDM-challenged *DNA-PKcs$^{fl/fl}$;* CD11c-Cre mice had reduced cell surface expression of the co-stimulatory molecule, CD80, which mediates signal 2 signaling via binding CD28 on T cells[49].

CD11b$^+$ DCs have been shown to be specialized for antigen presentation in the context of MHCII and induce Th2 responses via the expression of IRF4 (interferon regulatory factor-4) target genes, whereas CD11b$^-$ DCs, whose main function is to mediate MHCI-restricted cytotoxic T lymphocyte responses via the expression of IRF8 (IFN regulatory factor-8) and BATF3 (basic leucine zipper transcription factor, ATF-like 3), can prime MHCII-restricted T cell responses only at high doses of antigen[30]. Consistent with this, CD11b$^+$ DCs play an important role in mediating Th2 effector responses to HDM[28, 29]. CD11b$^+$ conventional DCs (cDCs) have been identified as the key DC subset that mediates the presentation of HDM antigens and the induction of Th2-mediated eosinophilic airway inflammation, whereas the primary role of CD11b$^+$ monocyte-derived DCs is to generate pro-inflammatory cytokines, although they can also induce Th2-mediated immunity to HDM[29]. Here, we show that CD11b$^+$ DCs that had been isolated from the MLNs of HDM-challenged *DNA-PKcs$^{fl/fl}$; CD11c^{Cre}* mice displayed impaired antigen presentation upon adoptive transfer to wild type mice that was associated with attenuated airway inflammation. This also demonstrates that the antigen presentation defect was not a consequence of deletion of DNA-PKcs in other CD11c$^+$ cells in the lung, such as alveolar macrophages. Furthermore, we found that neither uptake of HDM antigen nor subsequent migration to MLNs were impaired in CD11b$^+$ DCs from *DNA-PKcs$^{fl/fl}$;* CD11c-Cre mice. Collectively, these results demonstrate that DNA-PK-deficient CD11b$^+$ DCs have a defect in antigen presentation that results in attenuated allergic sensitization and Th2 immune responses to HDM.

IL-10 is an important anti-inflammatory cytokine that attenuates the functions of a variety of cell types that are relevant to the pathogenesis of asthma, including DCs[50, 51]. In particular, IL-10 suppresses several key DC functions, including antigen presentation, cellular maturation, expression of MHCII and co-stimulatory molecules, production of pro-inflammatory cytokines and activation of Akt and NF-κB signaling pathways[23, 50, 52].

Furthermore, mature pulmonary DCs can produce IL-10 in response to OVA challenge and thereby mediate antigen-specific T cell unresponsiveness indicative of immunologic tolerance, while IL-10 gene delivery to the lung suppresses Th2 inflammation, as well as antigen presentation and migration to MLNs by $CD11c^+$ DCs[53, 54]. Myeloid DCs have also been shown to produce IL-10 via TLR-dependent and TLR-independent pathways[51, 52, 55]. Here we show that in addition to defective antigen presentation by $CD11b^+$ DCs, HDM-challenged *DNA-PKcs*$^{fl/fl}$*; CD11c*-Cre mice had an increase in BALF levels of IL-10 and BMDCs from *DNA-PKcs*$^{fl/fl}$*;* CD11c-Cre mice secreted increased amounts of IL-10 in response to HDM. IL-10 production by BDMCs from wild type mice was increased following Akt inhibition, which is consistent with a ROS-activated pathway in HDM-stimulated DCs that signals via DNA-PK and Akt to attenuate IL-10 production. Thus, increases in IL-10 production may also contribute to the reduced allergic sensitization and Th2-type inflammation in HDM-challenged *DNA-PKcs*$^{fl/fl}$*; CD11c*^{Cre} mice.

We also assessed whether pharmacological inhibition of DNA-PK might represent an effective therapeutic approach to attenuate the manifestations of HDM-mediated allergic asthma. NU7441 (8-diebenzothiopen-4-yl-2-morpholin-4-yl-chromen-4-one) is a highly potent and selective, ATP-competitive inhibitor of DNA-PK (IC_{50} = 0.014 uM) that was initially identified by screening of a chromenone library[56]. NU7441 was developed as an anti-cancer agent based upon its ability to potentiate cell death mediated by chemotherapy- and radiation therapy-induced DSBs[57]. Here, we show that pharmacological inhibition of DNA-PK with NU7441 attenuated the induction of HDM-induced allergic sensitization, as well as Th2 effector cytokine production, airway inflammation, mucous cell metaplasia and AHR. Additionally, initiation of NU7441 treatment after T cell priming had already occurred similarly reduced HDM-induced airway inflammation, mucous cell metaplasia and AHR. Thus, we propose the concept of targeting DNA-PK with small molecule pharmacological inhibitors might be developed as a novel treatment approach for patients with allergic asthma. To avoid systemic effects, site-directed delivery of a DNA-PK inhibitor directly to the lungs via inhalation would likely represent the preferred method of administration.

To the best of our knowledge, our report is the first to describe a role for DNA-PK in modulating dendritic cell function in the pathogenesis of Th2 immune responses to HDM in experimental allergen-induced asthma. We propose that this is a novel and unexpected function for DNA-PK in DCs, as the adoptive transfer of $CD4^+$ T cells into *Prkdc*^{scid} mice has induced or enhanced disease in experimental murine models of colitis, skin allograft rejection and *Pneumocystis* pneumonia, which suggests that DC function in these settings is sufficient to mediate disease[58, 59, 60]. Additional studies will therefore be required to elucidate the dichotomy in DC function between experimental allergic asthma and other $CD4^+$ T cell-mediated disorders.

In summary, we have identified a novel function for DNA-PK in DCs where it is required for effective antigen presentation and the subsequent induction of allergic sensitization and Th2 immunity to HDM in the airway. We show that HDM induces phosphorylation and activation of DNA-PK via a ROS-dependent pathway and that ROS production by DCs is DNA-PK-dependent. Furthermore, we demonstrate that pharmacological inhibition of DNA-

PK with NU7441 attenuates the cardinal manifestations of experimental HDM-induced asthma, including allergic sensitization, Th2-mediated airway inflammation, mucous cell metaplasia and AHR. This identifies DNA-PK as a potential therapeutic target in asthma and can serve as the basis for the future development of DNA-PK inhibitors as a new treatment approach for patients with asthma.

Methods

Reagents

NU7441 was from Tocris Bioscience (Bristol, United Kingdom). DPI (diphenyleneiodonium chloride) and NAC (*N*-acetylcysteine) were from Calbiochem (EMD Millipore, Billerica, MA). House dust mite (*Dermatophagoides pteronyssinus*) extract was purchased from Greer Laboratories, Lenoir, NC as a freeze-dried preparation (Item #B82). The Akt inhibitors GDC0068 and MK2206 were from Cellagen Technology (San Jose, CA) and Selleckchem (Houston, TX), respectively. Quantikine ELISA kits for measurement of cytokines and chemokines were from R&D Systems (Minneapolis, MN).

Mice

BALB/c, C57BL/6, *Prkdc*^{scid} (CBySmn.CB17-*Prkdc*^{scid}), DO11.10 TCR (C.Cg-Tg(DO11.10)10Dlo), which express a transgenic MHC-II-restricted TCR that binds the ovalbumin (OVA) peptide antigen, OVA 323–339[24], and *Cd11c*-Cre (B6.Cg-Tg(Itgax-cre)1-1Reiz/J) mice were purchased from The Jackson Laboratories (Bar Harbor, Maine). 6 to 8 week old female mice were utilized for experiments. Murine experimental protocols were approved by the Animal Care and Use Committee of the National Heart, Lung, and Blood Institute, Bethesda, MD.

To generate the *DNA-PKcs*$^{fl/fl}$ mouse, a LoxP site was inserted between exons 81 and 82 of a 3.6 kb Hind III - SacI fragment of the mouse *Prkdc* gene in pBluescript II SK to give p1227 by using a Quikchange kit from Agilent Technologies (Santa Clara, CA) and oligo PKKpnLoxP2 (5′-CCTCCCAAGTGCTGGGATTAGGTACCATAACTTCGTATAATGTATGCTATACGAAGTTATAAGGCGTGCACTACCACTGC-3′). The insert resulting from the SacI digestion of p1227 was transferred into a SacI-digested plasmid pBSK-H3 that contained a 7.5 kb HindIII fragment of mouse *Prkdc* in pBluescript II SK, to generate plasmid p1228. A SalI - NotI fragment encoding FRT-Neo-FRT-Loxp from plasmid pL451 (http://ncifrederick.cancer.gov/research/brb/productDataSheets/recombineering/plasmid.aspx#PL451) was cloned between *Prkdc* exons 83 and 84 by PacI digestion of plasmid p1228[61]. The final construct was linearized by digestion with NotI for electroporation into the v6.5 mouse ES cell line (a 129 and C57BL/6J F1 hybrid ES cell line)[62]. Electroporated ES cells were grown in culture media containing both G418, for positive selection, and ganciclovir for negative selection. ES cell clones resistant to G418 and ganciclovir were screened for targeted insertion by southern blotting. ES cell clones with correct homologous recombination were injected into blastocyst-stage embryos, which were then transferred to the uteri of surrogate mothers. F0 generation mice born from the injected embryos are chimeras composed of genetic contributions from both the modified

ES cells and the recipient embryos. To obtain mouse lines that carry the gene-targeted mutation, we bred the chimeras to transmit the ES cell genetic component through the germ line. Once germ line transmission was established, mice were back-crossed to C57BL/6J mice for at least 10 generations. *DNA-PKcs*$^{fl/fl}$ mice were then bred with *CD11c*-Cre mice to generate *DNA-PKcs*$^{fl/fl}$*; CD11c*-Cre mice that were homozygous at each allele. Both male and female *DNA-PKcs*$^{fl/fl}$ and *DNA-PKcs*$^{fl/fl}$*; CD11c*-Cre mice that were 6 to 8 weeks old were utilized for experiments.

Southern blotting

An exon 79 probe labeled with ^{32}P by nick translation was used for Southern blotting to identify a 10 kb band for the modified *Prkdc* allele when genomic DNA was digested with EcoRI, while an exon 86 probe identified an 8.4 kb band when genomic DNA was digested with BamHI.

Genotyping and genomic sequencing

The following oligonucleotides, which flank the 5' LoxP of the targeting construct, were used as primers for PCR genotyping reactions; PKEx81f (5′-CTGGAGCCTATGTGCTAATGTACAG-3′) and PKEx82r (5′-CTGTTTCTGTACGGTTAGCTCGGCTG-3′). Genomic DNA was isolated from flow sorted cells using a DNAeasy kit (Qiagen) and PCR was performed using HotStar Taq (Qiagen). Amplification products were separated on 2% agarose gels that were stained with ethidium bromide to visualize a 646 bp band.

Genomic DNA from flow sorted cells was amplified by PCR using the following primers: NotpKEX81f (5′-GGGCGGCCGCCTGGAGCCTATGTGCTAATGTACAG-3′) and NotminusLoxPr (5′- GGGCGGCCGCGTGTCAGGTTTCATAACAATGCC-3′). Overlapping DNA sequences were obtained by PCR using the following primer pairs: PKseq30f (5′- GTTCTCTTGAGAGCTCTGGTCCG-3′) and PK Ex84seqr (5′-GGCATCAACTCAGGGACTGGAAG-3′), as well as NotpKEX81f and pKseq30r (5′-CGGACCAGAGCTCTCAAGAGAAC-3′). The amplified DNA was cloned and sequenced.

qRT-PCR

RNA was isolated from the same flow sorted cells using trizol reagent (Life Technologies, Grand Island, NY) and cDNA was generated using a High Capacity RNA-to-cDNA kit (Applied Biosystems). The cDNA was pre-amplified by PCR using oligos PKEx81f and PKEx83r (5′-CTGAGTAGCTGATCCAAACGC-3′) and HotStar Taq. qRT-PCR was performed in triplicate for each sample using a Taqman gene expression assay (Mm01342966_g1, Life Technologies, Grand Island, NY) that spans the junction between exons 82 and 83 of mouse *DNA-PKcs* and was normalized to 18S RNA. The assay was repeated three times.

Derivation of Dendritic cells from Monocytes and Bone Marrow Cells

Elutriated human monocytes, which had been obtained from normal volunteers who had provided informed consent to participate in an institutional review board-approved protocol (01-CC-0168), were provided by the Department of Transfusion Medicine, NIH Clinical

Center. Monocytes were cultured in RPMI 1640 medium containing 10% FBS, L-glutamine (2 mM), penicillin (100 U/ml), streptomycin (100 μg/ml) (Gibco®/Life Technologies, Grand Island, NY), human recombinant GM-CSF (150 ng/ml) and IL-4 (25 ng/ml) (BioLegend, San Diego, CA) in 10 cm petri dishes (BD Biosciences, San Jose, CA) for 7 days prior to experimentation to induce the differentiation of monocyte-derived dendritic cells (moDCs)[63]. $CD11c^+/HLA\text{-}DR^+/CD14^-$ human moDCs were analyzed by flow cytometry using the following antibodies, CD11c-APC, HLA-DR-PerCP/Cy5.5, CD14-Alexa Fluor® 488, CD40- Alexa Fluor® 647, CD80-Brilliant Violet 605™, and CD86-PE, all from Biolegend (San Diego, CA). Cell viability was assessed using Fixable Viability Dye eFluor® 450 (eBioscience, San Diego, CA).

Bone marrow cells were isolated from the leg bones of euthanized wild type and *Prkdc*^{scid} mice and cultured at a density of 2×10^6 cells/ml in RPMI 1640 medium containing 10% heat-inactivated FCS, penicillin (100 U/ml), streptomycin (100 μg/ml), L-glutamine (2 mM), 2-mercaptoethanol (50 μM), and recombinant mouse GM-CSF (20 ng/ml). Cultures were supplemented with an equal volume of medium on day 3 and 50% of the medium was replaced on day 6. Non-adherent cells were collected on day 8 and viable $CD11c^+$ bone marrow-derived dendritic cells (BMDCs) were sorted by flow cytometry using a CD11c-APC-Cy7 antibody from BD Biosciences (San Jose, CA). BMDCs were analyzed by flow cytometry using the following antibodies, CD11c-APC-eFluor 780, MHCII-PE-Cy7, CD40-APC, CD80-Cy5, CD86-eFluor 605 NC and Fixable Viability Dye eFluor® 450, all from eBioscience.

Western Blot Analysis

Human moDCs were lysed in RIPA buffer and 100 μg of protein that had been separated by SDS-PAGE using 4 – 20% Tris-Glycine gels (Lonza, Walkersville, MD) was transferred to nitrocellulose membranes (GE Healthcare Life Sciences, Pittsburgh, PA). Membranes were reacted with antibodies (1:1000 dilution) directed against phospho-DNA-PKcs (Ser2056) (Abcam, Cambridge, MA); DNA-PKcs (Thermo Scientific, Pittsburgh, PA); phospho-Akt (Ser473), phospho-Akt (Thr308), Akt (Cell Signaling Technology, Danvers, MA); and β-actin (Santa Cruz Biotechnology, Santa Cruz, CA). Blots were stripped using Restore Western Blot Stripping Buffer (Thermo Scientific).

Measurement of Intracellular Reactive Oxygen Species by Flow Cytometry

Cultures of human moDCs and BMDCs from WT C57BL6 and *Prkdc*^{SCID} mice were incubated with 2 μM of the redox-sensitive probe, CM-H_2DCFDA, (5-(and-6)-chloromethyl-2′,7′-dichlorodihydrofluorescein diacetate, acetyl ester) (Molecular Probes, Life Technologies, Grand Island, NY) for 30 min at 37°C. Oxidation of the CM-H_2DCFDA probe by reactive oxygen species (ROS) produces a stable fluorescent adduct that was detected by an increase of fluorescence in the fluorescein (FITC) channel. Levels of intracellular ROS generated in response to treatment with HDM (100 μg/ml) for 1 h were quantified by subtracting the background mean fluorescence intensity (MFI) of the non-fluorescent sample (negative control) from the measured MFI values of fluorescent samples in flow cytometry analysis.

OVA-induced T Cell Proliferation and Th2 Cytokine Production

BMDCs from WT BALB/c and *Prkdc*^{scid} mice were pulsed overnight with 1 μg/ml of OVA 323–339 peptide (AnaSpec, Fremont, CA) or PBS as a control and viable CD11c^{+} cells were isolated by flow sorting using an anti-mouse CD11c-APC-Cy7 antibody (BD Biosciences, San Jose, CA). Naïve CD4^{+} T cells were purified from the spleens of DO11.10 TCR mice by flow sorting using an anti-mouse CD4-eFluor® 650NC antibody (eBioscience, San Diego, CA) and labeled with 5 μM CFSE-SE (carboxyfluoroscein diacetate, succinimidyl ester) (Cayman Chemical, MI) for 30 mins. 1 × 10^{5} OVA peptide-specific CD4^{+} T cells were co-cultured with 2 × 10^{4} CD11c^{+} BMDCs in 96-well plates for 4 days and T cell proliferation was quantified by flow cytometry using the CSFE dye dilution method. The "Proliferation Ratio" is the MFI of CSFE-SE from OVA 323–339 peptide-pulsed CD11c^{+} BMDCs divided by the MFI of CSFE-SE from PBS-pulsed CD11c^{+} BMDCs. The quantity of IL-4, IL-5 and IL-13 released into the culture medium after 4 days was measured by ELISA.

For experiments assessing priming with full-length OVA, female BALB/c mice (6 – 8 weeks old) received intraperitoneal injections of ovalbumin (OVA; Sigma Aldrich, St. Louis, MO) emulsified in 0.2 ml of sterile PBS containing 2 mg of aluminum hydroxide (Sigma Aldrich) on days 0 and 7. 10^{5} splenic CD4^{+} T cells were purified by flow sorting on day 10, co-cultured with BMDCs from WT and *Prkdc*^{scid} mice at a 5:1 ratio in medium containing full-length OVA (1 μg/ml) for 4 days in 96-well plates and the quantity of cytokines released into the culture medium was measured by ELISA.

House Dust Mite Sensitization and Challenge Models

(1) Adoptive Transfer of CD11c^{+} Bone Marrow-derived Dendritic Cells from *Prkdc*^{scid} mice.CD11c^{+} bone marrow-derived DCs (BMDCs) that had been isolated from wild type and *Prkdc*^{scid} mice by flow cytometry were pulsed with HDM (100 μg/ml) or PBS for 16 h. 5 × 10^{4} viable CD11c^{+} BMDCs were adoptively transferred in 20 ul of PBS via intranasal administration on day 0 to recipient WT C57BL/6 mice. Recipient mice received daily intranasal HDM challenges (25 μg) on days 11 through 13 and endpoints were analyzed on day 15. The HDM extracts contained between 29.1 and 50 endotoxin units/mg of HDM protein, which resulted in 73 to 125 pg of LPS being administered with each 25 μg dose of HDM. **(2) Adoptive Transfer of CD11c^{+} Bone Marrow-derived Dendritic Cells Treated with NU7441 or GDC0068**. CD11c^{+} bone marrow-derived DCs (BMDCs) that had been isolated from wild type BALB/c mice by flow cytometry were pulsed with HDM (100 μg/ml) in the presence or absence of NU7441 (0.5 μM), GDC0068 (1 μM) or PBS for 16 h. 5 × 10^{4} viable CD11c^{+} BMDCs were adoptively transferred in 20 ul of PBS via intranasal administration on day 0 to recipient WT BALB/c mice. Recipient mice received daily intranasal HDM challenges (25 μg) on days 11 through 13 and endpoints were analyzed on day 15. **(3) Intranasal Sensitization and Challenge of *DNA-PKcs*$^{fl/fl}$ and *DNA-PKcs*$^{fl/fl}$*CD11c*^{Cre} mice**. *DNA-PKcs*$^{fl/fl}$ and *DNA-PKcs*$^{fl/fl}$*CD11c*^{Cre} mice were sensitized and challenged via daily intranasal administration of 25 μg of HDM or PBS, both in a volume of 10 μl, five days a week, for 6 weeks. **(4) Adoptive Transfer of CD11b^{+} Dendritic Cells Isolated from Mediastinal Lymph Nodes of HDM-pulsed DNA-PKcs$^{fl/fl}$ and DNA-PKcs$^{fl/fl;}$ *Cd11c*-Cre mice**. DCs from DNA-PKcs$^{fl/fl}$ and DNA-PKcs$^{fl/fl;}$ ***Cd11c***-

Cre mice were loaded *in vivo* with HDM allergen by intranasal instillation of HDM extract (100 μg), or saline as a control, using a modification of a previously described protocol[29]. After 4 days, mice were sacrificed, mediastinal lymph nodes were removed and $CD11c^+$/$CD11b^+$/$SiglecF^-$/$MHCII^+$ DCs were isolated from by flow cytometry using a FACS-ARIA II flow sorter (BD Biosciences, San Jose, CA) and the following antibodies, CD11c-APC-Cy7 and Siglec-F Alexa Fluor 647, both from BD Biosciences (San Jose, CA), CD11b–PerCP-Cy5.5 (eBioscience, San Diego, CA) and MHCII-PE-Cy7 from Biolegend (San Diego, CA). 2.5×10^4 $CD11c^+$/$CD11b^+$/$SiglecF^-$/$MHCII^+$ DCs were adoptively transferred to wild type C57BL/6 recipient mice by intranasal administration in a volume of 20 ul. All recipient mice received daily intranasal HDM challenges (25 μg) on days 9 through 14 and endpoints were analyzed on day 15. **(5) Oral Administration of NU7441**. Wild type BALB/c were sensitized and challenged by daily intranasal administration of HDM (25 ug) or PBS, both in a volume of 10 μl, five days a week for four weeks. Mice were fed chow that contained 0%, 0.6% or 0.9% NU7441 (TestDiet, St. Louis, MO) throughout the four week study period. For experiments assessing the effect of NU7441 administration only during the HDM challenge phase, WT BALB/c mice were sensitized by intraperitoneal injection of HDM (100 μg) emulsified in 200 μl of PBS containing 3 mg of aluminum hydroxide (Sigma-Aldrich) on days 0 and 4. Mice were challenged by intranasal administration of HDM (100 μg) in a volume of 40 μl on days 8, 10 and 12 and end-points were analyzed on day 14. Mice were fed chow that contained 0.9% NU7441 starting day 8, coincident with the start of the challenge phase of the protocol. Control mice were both sensitized and challenged with saline and were fed regular chow.

Analysis of Bronchoalveolar Lavage Fluid (BALF) and Lung Histopathology

Bronchoalveolar lavage was performed three times with 0.5 ml of PBS. Red blood cells were lysed with ACK buffer for 2 min at 4° C and cells were re-suspended in RPMI-1640 medium with 10% FBS. BALF cell counts were performed using a hemocytometer and differential cell counts were performed on Diff-Quik-stained cytospin slides (Siemens, Deerfield, Illinois). For histological analysis, lungs were inflated with 10% formalin to a pressure of 25 cm H_20, fixed in 10% formalin for 24 h, dehydrated through gradient ethanol, embedded in paraffin, sagittal sections cut to a thickness of 5 μm and stained with hematoxylin and eosin or periodic acid Schiff (PAS). Quantification of mucous cell metaplasia was performed by analyzing all the airways present (large (conducting), medium (central), and small (distal)) within each representative lung section. The number of airways that contained PAS-positive cells was counted and mucous cell metaplasia is presented as the percentage of airways with PAS-positive cells.

HDM-specific IgE

Plates were coated overnight with 0.01% HDM in PBS and blocked with 1% BSA in PBS prior to addition of serum samples that had been diluted 1:10 in blocking buffer and standards for 1h. Plates were washed 6x with PBS containing 0.05% Tween-20 prior to incubation with biotinylated anti-mouse IgE (Pharmingen, San Jose, CA) at a concentration of 2 μg/ml for 1 hr. Plates were washed an additional six times, streptavidin-HRP (R&D Systems, Minneapolis, MN) was added for 30 min and the amount of bound HDM-specific antibody was determined using TMB substrate.

Analysis of Cytokine Production by *ex vivo* Cultures of Mediastinal Lymph Node Cells Following *ex vivo* Re-stimulation with HDM

Single cell suspensions from mediastinal lymph nodes were cultured at a density 0.2×10^6 cells/ml in round-bottom 96-well plates and pulsed with HDM (100 μg/ml) for 72 hours at 37°C in RPMI medium containing 10 % FBS. In selected experiments, cells were also treated with NU7441 (0.5 μM).

Flow Cytometry

For genotyping of *DNA-PKcs*$^{fl/fl}$ and *DNA-PKcs*$^{fl/fl;}$ *CD11c*-Cre mice, CD11c$^+$/MHCII$^+$/SiglecF$^-$ DCs were isolated from spleens by flow sorting using a FACS-ARIA II flow cytometer (BD Biosciences, San Jose, CA) and the following antibodies, CD11c-APC-Cy7, MHCII-PE-Cy7 and SiglecF-AF647, all from BD Biosciences (San Jose, CA). Lung cells were isolated by enzymatic digestion using liberase (Roche, Indianapolis, IN), 100 μg/ml, and DNase I (Sigma-Aldrich, St Louis, MO), 0.2 mg/ml, in a volume of 1 to 2 ml per lung at 37 °C for 25 mins with agitation. Cells from digested lungs were incubated with anti-CD16/CD32 antibodies (clone 2.4G2) (Pharmingen/BD Biosciences, San Jose, CA) to block Fcγ III/II receptors before surface staining. Lung alveolar type II epithelial cells were isolated as CD45$^-$/CD11c$^-$/EpCAM$^+$ cells using the following antibodies, CD11c-APC-Cy7 and EpCAM-PE from BD Biosciences and CD45R-650NC, from eBioscience[64]. CD3$^+$ T cells and CD19$^+$ B cells present in the lungs and spleens of WT C57BL/6, DNA-PKcs$^{fl/fl}$ and DNA-PKcs$^{fl/fl;}$ *Cd11c*-Cre mice, were analyzed using CD3-APC and CD19-APC-Cy7, both from Biolegend, while the Fixable Viability Dye eFluor® 450 was from eBioscience. CD11c$^+$/MHC^{hi}/SSC^{lo} DCs present in lungs and mediastinal lymph nodes of HDM-challenged DNA-PKcs$^{fl/fl}$ and DNA-PKcs$^{fl/fl;}$ *Cd11c*-Cre mice were analyzed using the following anti-mouse antibodies, CD252 (OX40L)-PE, CD40-APC, CD80-PE-Cy5 and CD86 eFluor® 605NC, all from eBioscience (San Diego, CA). CD11b$^+$ DCs were identified using a CD11b–PerCPCy5.5 antibody (eBioscience), while TLR4 and TLR5 expression on CD11c$^+$/MHCII^{hi}/SSC^{lo}/CD11b$^+$ DCs were analyzed using TLR4-APC from Biolegend and TLR5-PE antibodies from Novus Biologics (Littleton, CO). Tregs were analyzed using CD3-APC, CD4-eFluor® 650NC, and CD25-PE-Cy7, all from eBiosciences. For quantification of intracellular Foxp3, cells were fixed and permeabilized with Foxp3 staining buffer and reacted with a Foxp3-PE antibody, both from eBioscience. All antibodies were utilized at a concentration of 0.5 – 1 μg/ml. Data were acquired on a LSRII (BD Biosciences, San Jose, CA) equipped with 407, 488, 532, and 633 LASER lines using DIVA 6.1.2 software and analyzed with the Flow Jo software version 9.6.1 (Treestar, San Carlos, CA). Cellular debris was excluded using a forward light scatter/side scatter plot.

For analysis of intracellular cytokines, 1×10^6 BAL cells/ml were suspended in RPMI-1640 supplemented with 10% FBS, L-glutamine (2 mM), penicillin (100 U/ml), and streptomycin (100 μg/ml), cultured in 24-well flat-bottom plates and stimulated with PMA (50 ng/ml), ionomycin (500 ng/ml) and brefeldin A (3 μg/ml) (eBiosciences) for 4 h at 37°C. Cells were washed with PBS, re-suspended in Flow Cytometry Staining Buffer (eBiosciences) containing 10% mouse serum (Jackson ImmunoResearch, Inc., West Grove, PA) and reacted with 5 μg/ml of rat anti-mouse CD3-APC-Cy7 and CD4-eFluor® 650NC for 30 mins, followed by two additional washes. Cells were treated with DNase I (60 μg/ml) for 15 mins

at 37°C, washed and re-suspended in 300 μl of permeabilization buffer containing 1% anti-mouse CD16/CD32 for 20 mins. Cells were then reacted with rat anti-mouse IL-5-PE, IL-13-APC, and IL-17-PE-Cy7 (eBiosciences) for 45 min at 4° C. Cells were washed twice with permeabilization buffer, re-suspended in PBS containing 1% paraformaldehyde and viable $CD3^{+/}CD4^{+}$ T cells that expressed IL-5, IL-13 or IL-17 were quantified using the LSR-II using FMO as controls by Flowjo analysis software.

Analysis of Dendritic Cell Migration to Mediastinal Lymph Nodes

50 μg of HDM that had been labeled with the Alexa Fluor® 647 (AF647) Protein Labeling Kit (Molecular Probes, Life Technologies, Grand Island, NY) was administered in 80 ul of PBS by i.t. instillation to *DNA-PKcs*$^{fl/fl}$ and *DNA-PKcs*$^{fl/fl}$*CD11c*^{Cre} mice[29]. Lungs and mediastinal lymph nodes were harvested after 72 hours and the number of $CD11c^{+}$/$MHCII^{hi}$/SSC^{lo}/$CD11b^{+}$/HDM^{+} DCs were quantified by flow cytometry.

Airway Hyperresponsiveness

Following cannulation of the trachea with a 19-gauge beveled metal catheter, airway resistance to increasing concentrations of methacholine (0 – 10 mg/ml) was directly measured in mechanically ventilated mice using an Elan RC Fine Pointe system (Buxco, Wilmington, NC) and average values are presented as cm H_2O/ml/s.

Statistics

Data were analyzed using Graph Pad Prism version 5.0a and are presented as mean ± SEM. A one-way ANOVA with Bonferroni's or Sidak's multiple comparison test, a Mann Whitney test or an unpaired *t* test were used for the analyses. A P value < 0.05 was considered significant.

Supplementary Material

Refer to Web version on PubMed Central for supplementary material.

Acknowledgements

Funding: Division of Intramural Research, National Heart, Lung, and Blood Institute.

We thank Dalton Saunders for his assistance with mouse management. The authors also thank Dr. Martha Vaughan and Dr. Joel Moss for their helpful discussions.

References

1. Davidson D, Amrein L, Panasci L, Aloyz R. Small Molecules, Inhibitors of DNA-PK, Targeting DNA Repair, and Beyond. Front Pharmacol. 2013; 4:5. [PubMed: 23386830]
2. Kong X, Shen Y, Jiang N, Fei X, Mi J. Emerging roles of DNA-PK besides DNA repair. Cell Signal. 2011; 23:1273–1280. [PubMed: 21514376]
3. Meek K, Dang V, Lees-Miller SP. DNA-PK: the means to justify the ends? Adv Immunol. 2008; 99:33–58. [PubMed: 19117531]
4. Chen BP, Li M, Asaithamby A. New insights into the roles of ATM and DNA-PKcs in the cellular response to oxidative stress. Cancer Lett. 2012; 327:103–110. [PubMed: 22155347]

5. Neal JA, Meek K. Choosing the right path: does DNA-PK help make the decision? Mutat Res. 2011; 711:73–86. [PubMed: 21376743]
6. Ma Y, Pannicke U, Schwarz K, Lieber MR. Hairpin opening and overhang processing by an Artemis/DNA-dependent protein kinase complex in nonhomologous end joining and V(D)J recombination. Cell. 2002; 108:781–794. [PubMed: 11955432]
7. Blunt T, et al. Defective DNA-dependent protein kinase activity is linked to V(D)J recombination and DNA repair defects associated with the murine scid mutation. Cell. 1995; 80:813–823. [PubMed: 7889575]
8. Bosma GC, Custer RP, Bosma MJ. A severe combined immunodeficiency mutation in the mouse. Nature. 1983; 301:527–530. [PubMed: 6823332]
9. Dorshkind K, et al. Functional status of cells from lymphoid and myeloid tissues in mice with severe combined immunodeficiency disease. J Immunol. 1984; 132:1804–1808. [PubMed: 6607948]
10. Jhappan C, Morse HC 3rd, Fleischmann RD, Gottesman MM, Merlino G. DNA-PKcs: a T-cell tumour suppressor encoded at the mouse scid locus. Nat Genet. 1997; 17:483–486. [PubMed: 9398856]
11. Blunt T, et al. Identification of a nonsense mutation in the carboxyl-terminal region of DNA-dependent protein kinase catalytic subunit in the scid mouse. Proc Natl Acad Sci U S A. 1996; 93:10285–10290. [PubMed: 8816792]
12. Danska JS, Holland DP, Mariathasan S, Williams KM, Guidos CJ. Biochemical and genetic defects in the DNA-dependent protein kinase in murine scid lymphocytes. Mol Cell Biol. 1996; 16:5507–5517. [PubMed: 8816463]
13. Taccioli GE, et al. Targeted disruption of the catalytic subunit of the DNA-PK gene in mice confers severe combined immunodeficiency and radiosensitivity. Immunity. 1998; 9:355–366. [PubMed: 9768755]
14. Ferguson BJ, Mansur DS, Peters NE, Ren H, Smith GL. DNA-PK is a DNA sensor for IRF-3-dependent innate immunity. Elife. 2012; 1:e00047. [PubMed: 23251783]
15. Peters NE, et al. A mechanism for the inhibition of DNA-PK-mediated DNA sensing by a virus. PLoS Pathog. 2013; 9:e1003649. [PubMed: 24098118]
16. Cooper A, Garcia M, Petrovas C, Yamamoto T, Koup RA, Nabel GJ. HIV-1 causes CD4 cell death through DNA-dependent protein kinase during viral integration. Nature. 2013; 498:376–379. [PubMed: 23739328]
17. Leitao E, et al. Listeria monocytogenes induces host DNA damage and delays the host cell cycle to promote infection. Cell Cycle. 2014; 13:928–940. [PubMed: 24552813]
18. Rajagopalan S, Moyle MW, Joosten I, Long EO. DNA-PKcs controls an endosomal signaling pathway for a proinflammatory response by natural killer cells. Sci Signal. 2010; 3 ra14.
19. Ju J, et al. Phosphorylation of p50 NF-kappaB at a single serine residue by DNA-dependent protein kinase is critical for VCAM-1 expression upon TNF treatment. J Biol Chem. 2010; 285:41152–41160. [PubMed: 20966071]
20. Kwan HY, Fong WF, Yang Z, Yu ZL, Hsiao WL. Inhibition of DNA-dependent protein kinase reduced palmitate and oleate-induced lipid accumulation in HepG2 cells. European Journal of Nutrition. 2013; 52:1621–1630. [PubMed: 23184344]
21. Yu M, Lam J, Rada B, Leto TL, Levine SJ. Double-stranded RNA induces shedding of the 34-kDa soluble TNFR1 from human airway epithelial cells via TLR3-TRIF-RIP1-dependent signaling: roles for dual oxidase 2- and caspase-dependent pathways. J Immunol. 2011; 186:1180–1188. [PubMed: 21148036]
22. Chen BP, et al. Cell cycle dependence of DNA-dependent protein kinase phosphorylation in response to DNA double strand breaks. J Biol Chem. 2005; 280:14709–14715. [PubMed: 15677476]
23. Bhattacharyya S, Sen P, Wallet M, Long B, Baldwin AS Jr, Tisch R. Immunoregulation of dendritic cells by IL-10 is mediated through suppression of the PI3K/Akt pathway and of IkappaB kinase activity. Blood. 2004; 104:1100–1109. [PubMed: 15113757]
24. Murphy KM, Heimberger AB, Loh DY. Induction by antigen of intrathymic apoptosis of CD4+CD8+TCRlo thymocytes in vivo. Science. 1990; 250:1720–1723. [PubMed: 2125367]

25. Barnes PJ. The cytokine network in asthma and chronic obstructive pulmonary disease. J Clin Invest. 2008; 118:3546–3556. [PubMed: 18982161]
26. Campbell JJ, et al. Expression of chemokine receptors by lung T cells from normal and asthmatic subjects. J Immunol. 2001; 166:2842–2848. [PubMed: 11160352]
27. Ruis BL, Fattah KR, Hendrickson EA. The catalytic subunit of DNA-dependent protein kinase regulates proliferation, telomere length, and genomic stability in human somatic cells. Mol Cell Biol. 2008; 28:6182–6195. [PubMed: 18710952]
28. Mesnil C, et al. Resident CD11b(+)Ly6C(−) lung dendritic cells are responsible for allergic airway sensitization to house dust mite in mice. PLoS One. 2012; 7:e53242. [PubMed: 23300898]
29. Plantinga M, et al. Conventional and monocyte-derived CD11b(+) dendritic cells initiate and maintain T helper 2 cell-mediated immunity to house dust mite allergen. Immunity. 2013; 38:322–335. [PubMed: 23352232]
30. Vander Lugt B, et al. Transcriptional programming of dendritic cells for enhanced MHC class II antigen presentation. Nat Immunol. 2014; 15:161–167. [PubMed: 24362890]
31. Wu J, et al. DNA-PKcs interacts with Aire and regulates the expression of toll-like receptors in RAW264.7 cells. Scand J Immunol. 2012; 75:479–488. [PubMed: 22239103]
32. Hammad H, Chieppa M, Perros F, Willart MA, Germain RN, Lambrecht BN. House dust mite allergen induces asthma via Toll-like receptor 4 triggering of airway structural cells. Nat Med. 2009; 15:410–416. [PubMed: 19330007]
33. Wilson RH, et al. The Toll-like receptor 5 ligand flagellin promotes asthma by priming allergic responses to indoor allergens. Nat Med. 2012; 18:1705–1710. [PubMed: 23064463]
34. Lambrecht BN, Hammad H. Lung dendritic cells in respiratory viral infection and asthma: from protection to immunopathology. Annu Rev Immunol. 2012; 30:243–270. [PubMed: 22224777]
35. Hammad H, et al. Inflammatory dendritic cells--not basophils--are necessary and sufficient for induction of Th2 immunity to inhaled house dust mite allergen. J Exp Med. 2010; 207:2097–2111. [PubMed: 20819925]
36. Hemmi H, Kaisho T, Takeda K, Akira S. The roles of Toll-like receptor 9, MyD88, and DNA-dependent protein kinase catalytic subunit in the effects of two distinct CpG DNAs on dendritic cell subsets. J Immunol. 2003; 170:3059–3064. [PubMed: 12626561]
37. Ishii KJ, et al. Potential role of phosphatidylinositol 3 kinase, rather than DNA-dependent protein kinase, in CpG DNA-induced immune activation. J Exp Med. 2002; 196:269–274. [PubMed: 12119352]
38. Ma C, Muranyi M, Chu CH, Zhang J, Chu WM. Involvement of DNA-PKcs in the IL-6 and IL-12 response to CpG-ODN is mediated by its interaction with TRAF6 in dendritic cells. PLoS One. 2013; 8:e58072. [PubMed: 23533581]
39. Bouquet F, et al. A DNA-dependent stress response involving DNA-PK occurs in hypoxic cells and contributes to cellular adaptation to hypoxia. J Cell Sci. 2011; 124:1943–1951. [PubMed: 21576354]
40. Rocourt CR, Wu M, Chen BP, Cheng WH. The catalytic subunit of DNA-dependent protein kinase is downstream of ATM and feeds forward oxidative stress in the selenium-induced senescence response. J Nutr Biochem. 2013; 24:781–787. [PubMed: 22841545]
41. Zhang X, Zhu Y, Geng L, Wang H, Legerski RJ. Artemis is a negative regulator of p53 in response to oxidative stress. Oncogene. 2009; 28:2196–2204. [PubMed: 19398950]
42. Feng J, Park J, Cron P, Hess D, Hemmings BA. Identification of a PKB/Akt hydrophobic motif Ser-473 kinase as DNA-dependent protein kinase. J Biol Chem. 2004; 279:41189–41196. [PubMed: 15262962]
43. Bozulic L, Surucu B, Hynx D, Hemmings BA. PKBalpha/Akt1 acts downstream of DNA-PK in the DNA double-strand break response and promotes survival. Mol Cell. 2008; 30:203–213. [PubMed: 18439899]
44. Matsue H, et al. Generation and function of reactive oxygen species in dendritic cells during antigen presentation. J Immunol. 2003; 171:3010–3018. [PubMed: 12960326]
45. Maemura K, et al. Reactive oxygen species are essential mediators in antigen presentation by Kupffer cells. Immunol Cell Biol. 2005; 83:336–343. [PubMed: 16033528]

46. Kotsias F, Hoffmann E, Amigorena S, Savina A. Reactive oxygen species production in the phagosome: impact on antigen presentation in dendritic cells. Antioxid Redox Signal. 2013; 18:714–729. [PubMed: 22827577]
47. Sevin CM, et al. Deficiency of gp91phox Inhibits Allergic Airway Inflammation. Am J Respir Cell Mol Biol. 2013; 49:396–402. [PubMed: 23590311]
48. Tang H, et al. The T helper type 2 response to cysteine proteases requires dendritic cell-basophil cooperation via ROS-mediated signaling. Nat Immunol. 2010; 11:608–617. [PubMed: 20495560]
49. Reis e Sousa C. Dendritic cells in a mature age. Nat Rev Immunol. 2006; 6:476–483. [PubMed: 16691244]
50. Hawrylowicz CM, O'Garra A. Potential role of interleukin-10-secreting regulatory T cells in allergy and asthma. Nat Rev Immunol. 2005; 5:271–283. [PubMed: 15775993]
51. Saraiva M, O'Garra A. The regulation of IL-10 production by immune cells. Nat Rev Immunol. 2010; 10:170–181. [PubMed: 20154735]
52. Chang J, Kunkel SL, Chang CH. Negative regulation of MyD88-dependent signaling by IL-10 in dendritic cells. Proceedings of the National Academy of Sciences of the United States of America. 2009; 106:18327–18332. [PubMed: 19815506]
53. Akbari O, DeKruyff RH, Umetsu DT. Pulmonary dendritic cells producing IL-10 mediate tolerance induced by respiratory exposure to antigen. Nat Immunol. 2001; 2:725–731. [PubMed: 11477409]
54. Nakagome K, et al. In vivo IL-10 gene delivery suppresses airway eosinophilia and hyperreactivity by down-regulating APC functions and migration without impairing the antigen-specific systemic immune response in a mouse model of allergic airway inflammation. J Immunol. 2005; 174:6955–6966. [PubMed: 15905538]
55. Geijtenbeek TB, et al. Mycobacteria target DC-SIGN to suppress dendritic cell function. The Journal of Experimental Medicine. 2003; 197:7–17. [PubMed: 12515809]
56. Leahy JJ, et al. Identification of a highly potent and selective DNA-dependent protein kinase (DNA-PK) inhibitor (NU7441) by screening of chromenone libraries. Bioorg Med Chem Lett. 2004; 14:6083–6087. [PubMed: 15546735]
57. Zhao Y, et al. Preclinical evaluation of a potent novel DNA-dependent protein kinase inhibitor NU7441. Cancer Res. 2006; 66:5354–5362. [PubMed: 16707462]
58. Roopenian DC, Anderson PS. Adoptive immunity in immune-deficient scid/scid mice. I. Differential requirements of naive and primed lymphocytes for CD4+ T cells during rejection of minor histocompatibility antigen-disparate skin grafts. Transplantation. 1988; 46:899–904. [PubMed: 2905088]
59. Roths JB, Sidman CL. Both immunity and hyperresponsiveness to Pneumocystis carinii result from transfer of CD4+ but not CD8+ T cells into severe combined immunodeficiency mice. J Clin Invest. 1992; 90:673–678. [PubMed: 1353767]
60. Mudter J, Wirtz S, Galle PR, Neurath MF. A new model of chronic colitis in SCID mice induced by adoptive transfer of CD62L+ CD4+ T cells: insights into the regulatory role of interleukin-6 on apoptosis. Pathobiology. 2002; 70:170–176. [PubMed: 12571422]
61. Liu P, Jenkins NA, Copeland NG. A highly efficient recombineering-based method for generating conditional knockout mutations. Genome Res. 2003; 13:476–484. [PubMed: 12618378]
62. Eggan K, et al. Hybrid vigor, fetal overgrowth, and viability of mice derived by nuclear cloning and tetraploid embryo complementation. Proc Natl Acad Sci U S A. 2001; 98:6209–6214. [PubMed: 11331774]
63. Akagawa KS, et al. Generation of CD1+RelB+ dendritic cells and tartrate-resistant acid phosphatase-positive osteoclast-like multinucleated giant cells from human monocytes. Blood. 1996; 88:4029–4039. [PubMed: 8916970]
64. Messier EM, Mason RJ, Kosmider B. Efficient and rapid isolation and purification of mouse alveolar type II epithelial cells. Experimental Lung Research. 2012; 38:363–373. [PubMed: 22888851]

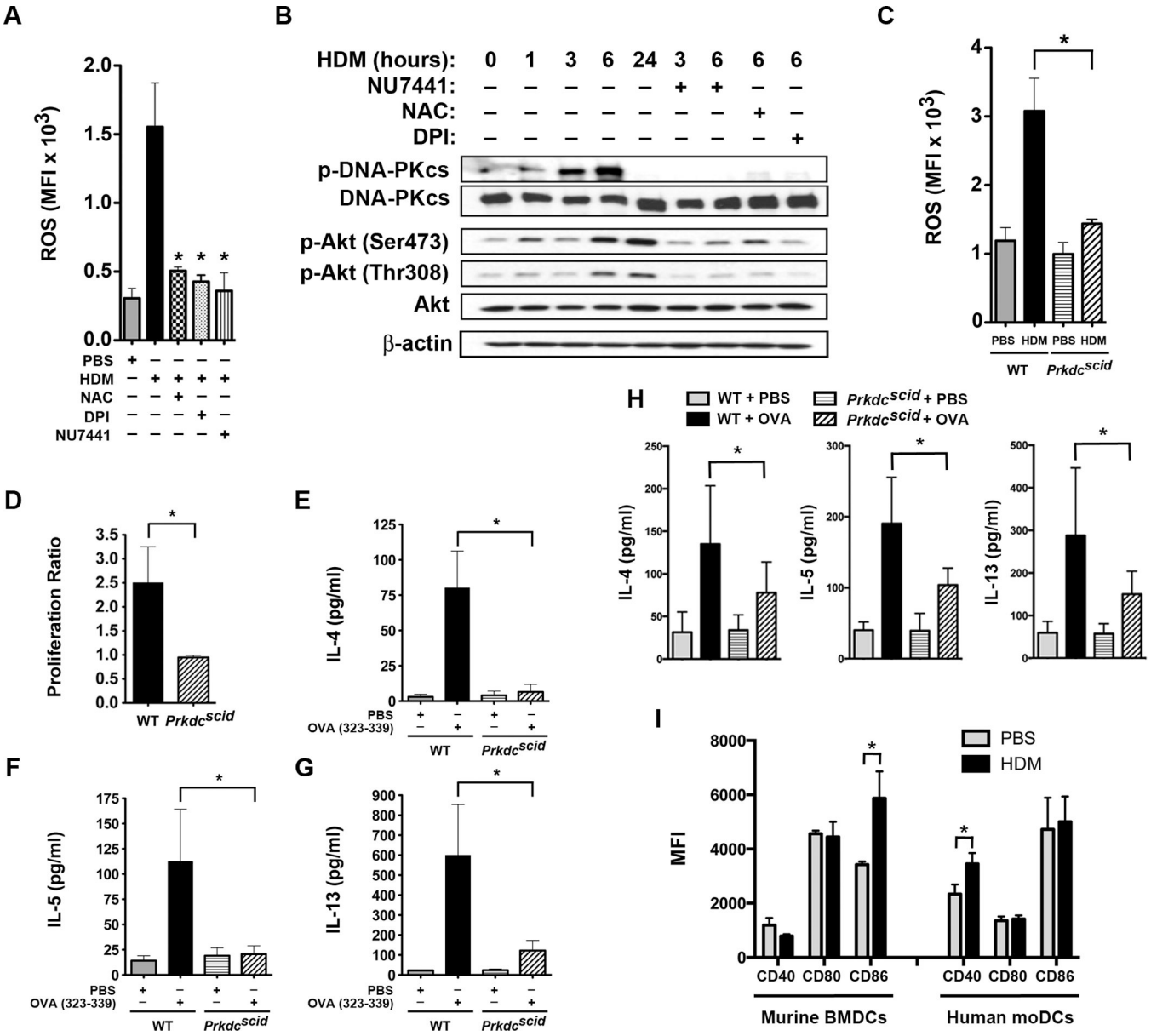

Figure 1. House Dust Mite induces Phosphorylation of Dendritic Cell DNA-PK via Generation of Reactive Oxygen Species

A. Mean fluorescence intensity (MFI) of intracellular reactive oxygen species (ROS) generated by human monocyte-derived dendritic cells (moDC) stimulated with house dust mite (HDM) (100 μg/ml) for 1 h with or without NAC (2 mM), DPI (10 μM) or NU7441 (0.5 μM) (n = 3 – 5, * P< 0.01 vs. HDM, one way ANOVA with Bonferroni multiple comparison test). **B**. Western blots of HDM-stimulated human moDC proteins with or without NU7441, NAC or DPI for 1 to 24 h (see Supplementary Figure 2 for images of full original blots). Image is representative of 4 blots. **C**. MFI of intracellular ROS generated by bone marrow-derived dendritic cells (BMDC) from wild type (WT) and *Prkdc*^{scid} mice stimulated with HDM (100 μg/ml) for 1 h (n = 3, * P< 0.01, WT + HDM vs. *Prkdc*^{scid} + HDM, one way ANOVA with Bonferroni multiple comparison test). **D**. CD11c^{+} BMDC

from *Prkdc*^{scid} and WT mice were pulsed with the ovalbumin (OVA) 323–339 peptide and incubated at a 1:5 ratio with CSFE-labeled CD4$^+$ DO11.10 T cells for 4 days. OVA-specific proliferation is presented as proliferation index (n = 8, * P = 0.0011, Mann Whitney test, pooled data from 3 independent experiments). **E – G**. Th2 cytokines released by co-cultures of OVA 323–329-pulsed BMDCs and CSFE-labeled DO11.10 CD3$^+$/CD4$^+$ T cells (n = 3, *P < 0.05, WT + OVA vs. *Prkdc*^{scid} + OVA, one way ANOVA with Bonferroni multiple comparison test). **H**. Co-cultures of BMDCs from *Prkdc*^{scid} and WT mice incubated at a 1:5 ratio with splenic CD4$^+$ T cells from WT mice sensitized to full-length OVA. Co-cultures were treated with PBS or OVA (1 μg/ml) for 4 days and Th2 cytokines were quantified (n = 7, * P < 0.05). Pooled data from 2 independent experiments. **I**. MFI of CD40, CD80 and CD86 cell surface expression by murine BMDCs (n = 6 mice) and human moDCs (n = 10 mice) stimulated with or without HDM (100 μg/ml) for 24 h. Pooled data from 2 independent experiments (* P < 0.05, Mann Whitney test).

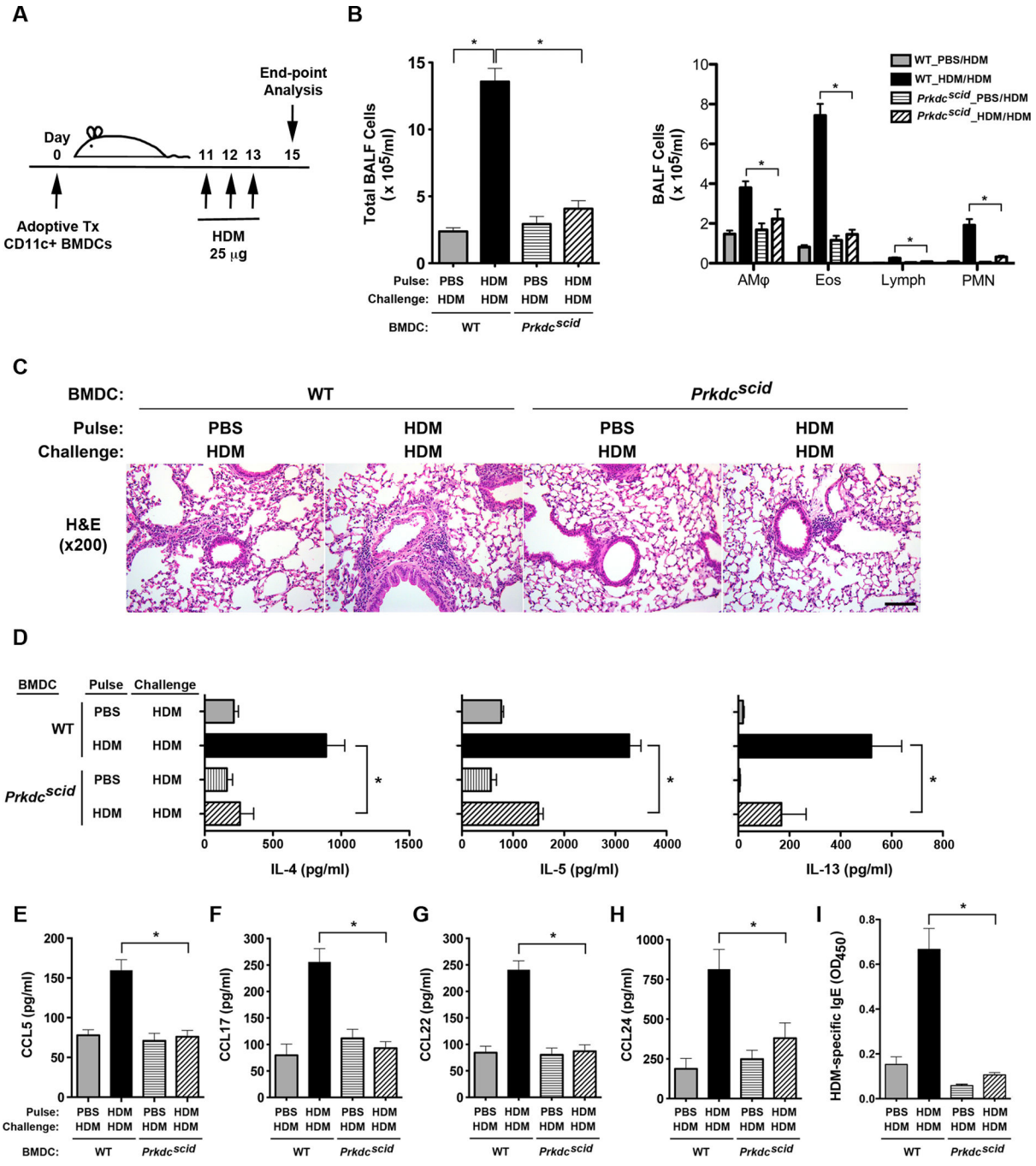

Figure 2. The Adoptive Transfer of HDM-pulsed CD11c$^+$ Bone Marrow-derived Dendritic Cells from *Prkdc^{scid}* mice has a Reduced Ability to Induce Allergen-mediated Airway Inflammation

A. On day 0, 5 × 10^4 viable CD11c$^+$ bone marrow-derived dendritic cells (BMDCs) from wild type C57BL/6 and *Prkdc^{scid}*mice, which had been pulsed *ex vivo* with HDM or PBS, as a control, were adoptively transferred to recipient wild type C57BL/6 mice. Daily intranasal HDM challenges (25 μg) were administered to all recipient mice on days 11 through 13 and endpoints were analyzed on day 15. **B**. Number of total BALF inflammatory cells and inflammatory cell types (alveolar macrophages (AMφ), eosinophils (Eos), lymphocytes

(Lymph) and neutrophils (PMN)) from HDM-challenged mice that had received the adoptive transfer of 5×10^4 $CD11c^+$ BMDCs from *Prkdc*^{scid} and wild type mice that had been pulsed with either PBS or HDM (n = 12 – 14 mice, * $P < 0.01$, one way ANOVA with Bonferroni multiple comparison test). **C**. Representative histologic lung sections from HDM-challenged mice that had received the adoptive transfer of $CD11c^+$ BMDCs from *Prkdc*^{scid} and wild type mice. The scale bar denotes 100 μm. **D**. Th2 cytokine secretion by *ex vivo* cultures of mediastinal lymph node cells that had been re-stimulated with or without HDM (100 μg/ml) (n = 3 – 8 mice, * $P < 0.05$, one way ANOVA with Bonferroni multiple comparison test). One of two independent experiments that showed similar results is shown (data were not pooled due to different ranges of cytokine production between the two experiments). **E – H**. C-C chemokines in BALF (n = 11 – 13 mice, *$P< 0.01$, one way ANOVA with Bonferroni multiple comparison test). **I**. Serum house dust mite-specific IgE (n = 8 – 16 mice, * $P < 0.0001$, one way ANOVA with Bonferroni multiple comparison test). Results are pooled data from two independent experiments, except where indicated.

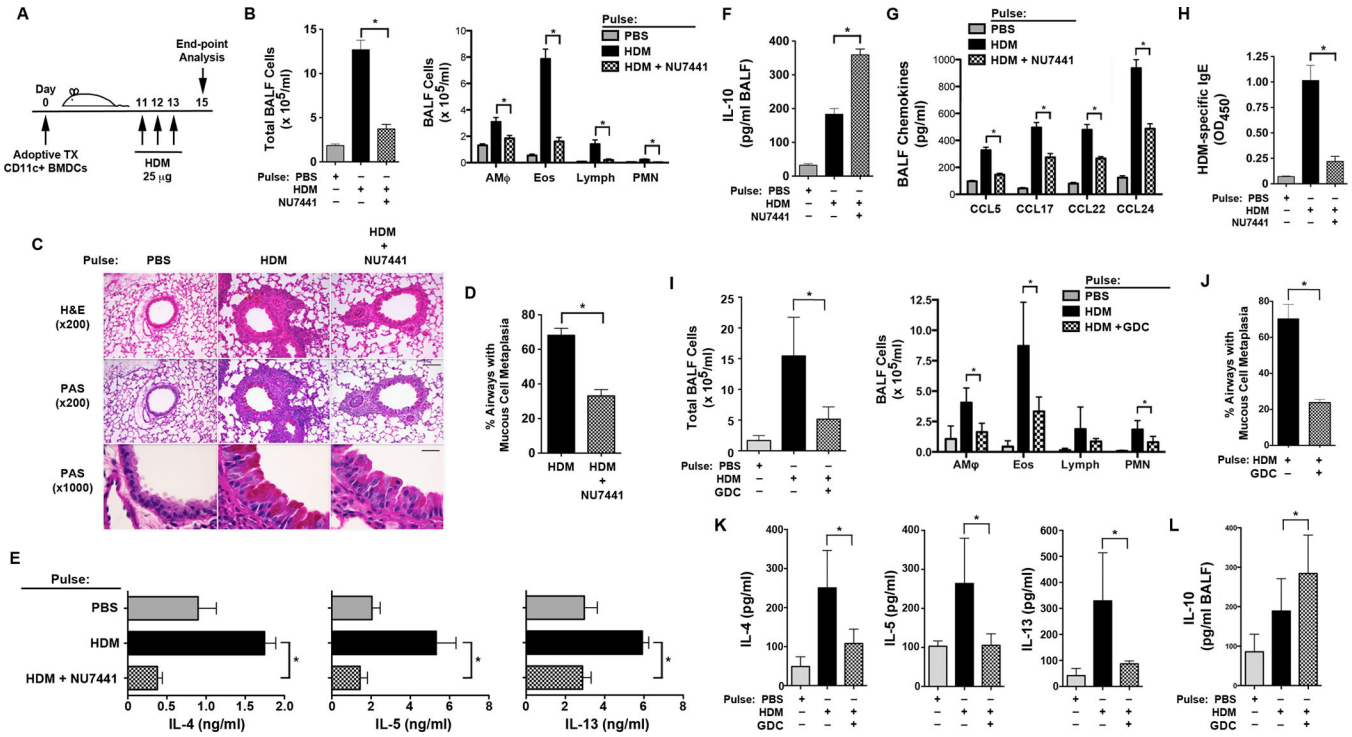

Figure 3. The Adoptive Transfer of HDM-pulsed CD11c$^+$ Bone Marrow-derived Dendritic Cells Treated with the DNA-PK inhibitor, NU7441, or the Akt inhibitor, GDC0068, have an Impaired Ability to Induce Allergen-mediated Airway Inflammation

A. On day 0, 5×10^4 viable CD11c$^+$ bone marrow-derived dendritic cells (BMDCs) from wild type (WT) C57BL/6 mice that were pulsed *ex vivo* with HDM (100 μg/ml) or PBS, with or without 0.5 μM NU7441 (Panels A – H) or 1 μM GDC0068 (Panels I – L), were adoptively transferred to recipient WT mice. Daily intranasal HDM challenges (25 μg) were administered to all recipient mice on days 11 through 13 and endpoints were analyzed on day 15. **B**. Number of total BALF cells and inflammatory cell types (alveolar macrophages (AMφ), eosinophils (Eos), lymphocytes (Lymph) and neutrophils (PMN)) from HDM-challenged mice that had received the adoptive transfer of CD11c$^+$ BMDCs treated with NU7441 and pulsed with either PBS or HDM (n = 12 mice, * P < 0.01, one way ANOVA with Bonferroni multiple comparison test). **C**. Representative histologic lung sections stained with hematoxylin and eosin (H&E) or periodic acid-Schiff (PAS). Scale bars denote 100 μm for the x200 images and 20 μm for the x1000 images. **D**. Quantification of mucous cell metaplasia. (n = 12 mice, *P < 0.0001, HDM + NU7441 vs. HDM alone, Mann Whitney test). 54 + 3 airways were examined per mouse. **E**. Th2 cytokine secretion by *ex vivo* cultures of mediastinal lymph node cells that had been re-stimulated with PBS or HDM (100 μg/ml) (n = 9 – 16 mice, * P < 0.01, HDM vs. HDM+NU7441, one way ANOVA with Bonferroni multiple comparison test). **F**. BALF IL-10 (n = 12 mice, * P < 0.0001, HDM vs. HDM+NU7441, one way ANOVA with Bonferroni multiple comparison test). **G**. BALF C-C chemokines (n = 12 mice, * P < 0.0001, HDM vs. HDM+NU7441, one way ANOVA with Bonferroni multiple comparison test). **H**. Serum HDM-specific IgE (n = 8 – 15 mice, * P < 0.001, HDM vs. HDM+NU7441, one way ANOVA with Bonferroni multiple comparison test). **I**. Number of BALF inflammatory cells from HDM-challenged mice that

received the adoptive transfer of $CD11c^+$ BMDCs treated with the Akt inhibitor, GDC0068 (GDC), and pulsed with either PBS or HDM (n = 8 – 9 mice, * P < 0.001, one way ANOVA with Sidak's multiple comparison test). **J**. Quantification of mucous cell metaplasia. (n = 5 mice, *P = 0.0079, HDM + GDC0068 (GDC) vs. HDM alone, Mann Whitney test). 65 + 2 airways were examined per mouse. **K**. Th2 cytokine secretion by *ex vivo* cultures of mediastinal lymph node cells that were re-stimulated with PBS or HDM (100 μg/ml) (n = 4 mice, * P < 0.05, HDM vs. HDM+GDC0068, one way ANOVA with Sidak's multiple comparison test). Representative results from one of two independent experiments are shown. **L**. BALF IL-10 (n = 9 mice, * P < 0.05, HDM vs. HDM+GDC0068, one way ANOVA with Sidak's multiple comparison test). Results are pooled data from two independent experiments, unless otherwise indicated.

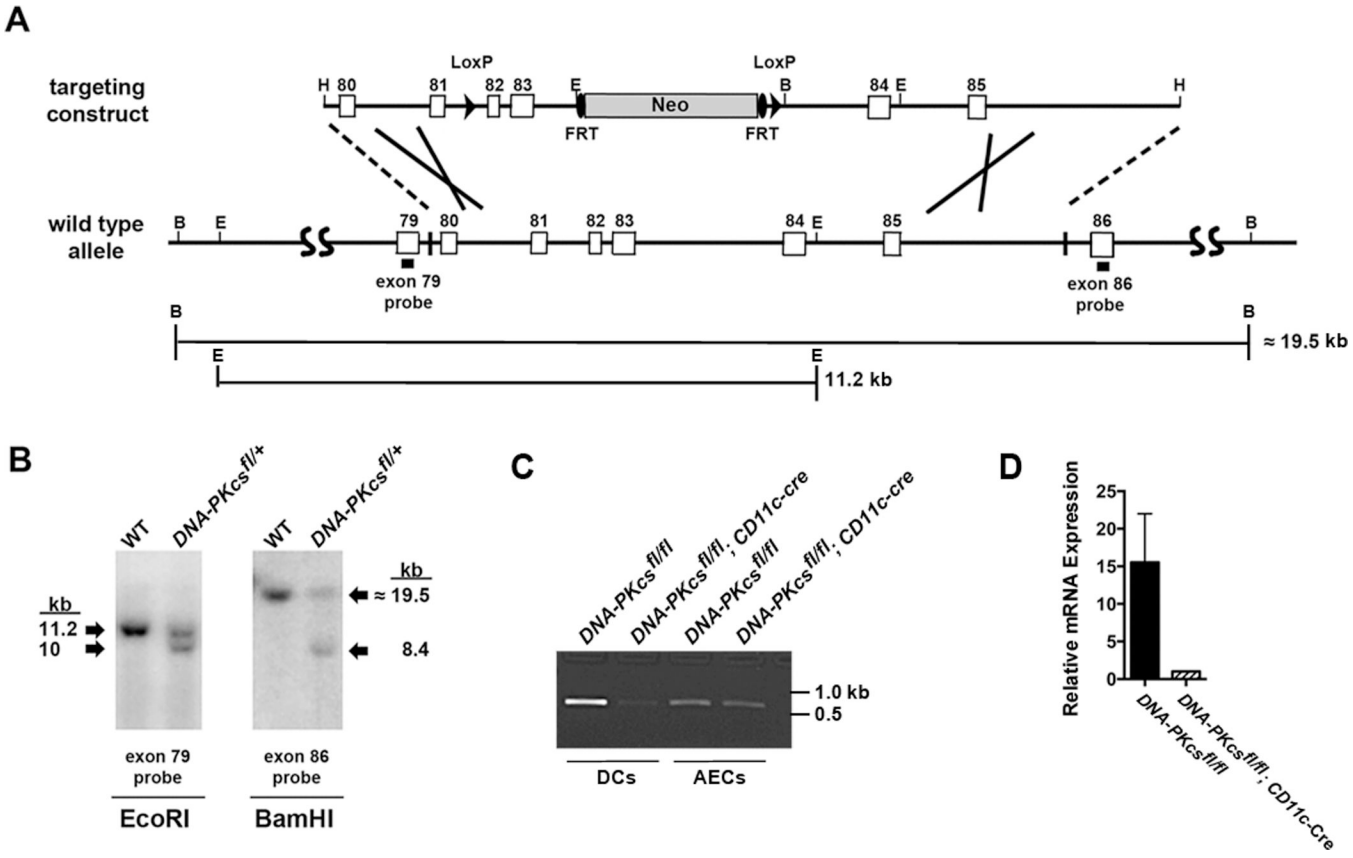

Figure 4. Generation and characterization of *DNA-PKcs*$^{fl/fl}$*; CD11c-Cre* mice

A, The *DNA-PKcs*$^{fl/fl}$ targeting construct, consisting of a HindIII fragment containing exons 80 to 85 of the mouse *Prkdc gene*, is shown at the top while the wild type allele is shown below for comparison. LoxP is shown as an arrowhead, Neo is shown as a cylinder and FRT is shown as an oval. Restriction sites located at the ends of the construct or used in Southern blotting are indicated (H, HindIII; B, BamHI; E, EcoRI). The exon 79 and exon 86 probes used in Southern blotting are shown by solid rectangles. The sizes of the fragments following digestion of the native *Prkdc* gene with BamHI or EcoRI are indicated. **B**. Southern blots of genomic DNA from WT and *DNA-PKcs*$^{fl/+}$mice. Left panel, digestion with EcoRI and detection with an exon 79 probe. Right panel, digestion with BamHI and detection with an exon 86 probe. **C**. Genomic DNA from CD11c^{+}/MHCII^{+}/SiglecF^{-} splenic dendritic cells and CD11c^{-}/CD45^{-}/Ep-CAM^{+} alveolar type II cells isolated from the lungs of *DNA-PKcs*$^{fl/fl}$ and *DNA-PKcs*$^{fl/fl}$*; CD11c*-Cre mice by flow cytometry. PCR was performed using exon 81 (PKEx81f) and exon 82 (PKEx82r) primers that flank the 5′ loxP site to generate a 646 bp product from the floxed allele, but not from the recombined allele. (See Supplementary Figures 3 and 4 for full original images of Panels B and C.) **D**. CD11c^{+}/MHCII^{+}/SiglecF^{-} splenic dendritic cells from *DNA-PKcs*$^{fl/fl}$ and *DNA-PKcs*$^{fl/fl}$*; CD11c*-Cre mice were sorted by flow cytometry. qRT-PCR was performed on pre-amplified cDNA using a Taqman assay that spanned the junction between exons 82 and 83 of *DNA-PKcs* mRNA (each sample represents pooled cells from 5 mice).

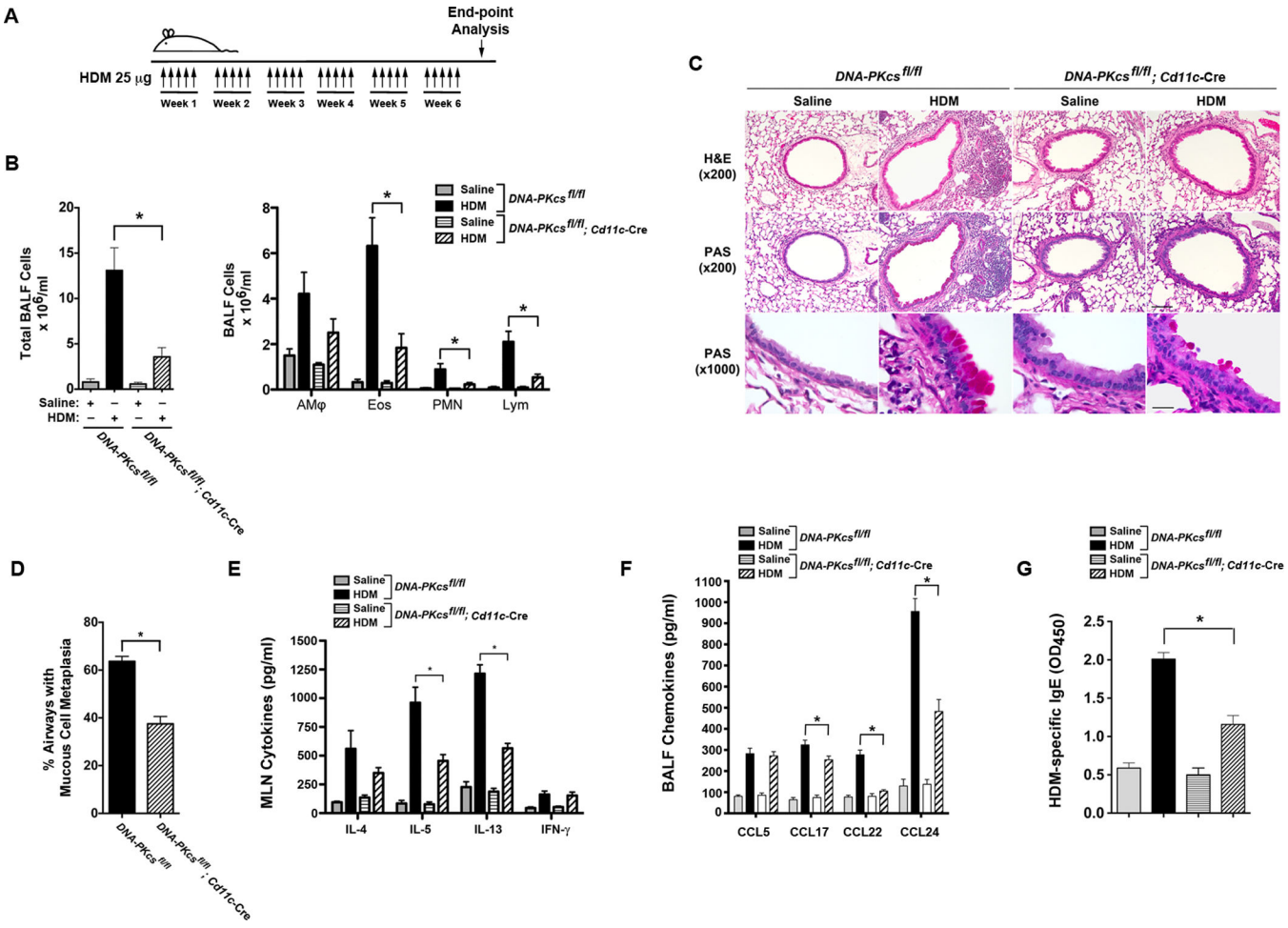

Figure 5. HDM-challenged CD11c-specific *DNA-PKcs* Knockout Mice Have Impaired Allergen-mediated Inflammation

A. *DNA-PKcs*$^{fl/fl}$ and *DNA-PKcs*$^{fl/fl}$*; CD11c-Cre* mice were sensitized and challenged by daily administration of HDM 25 micrograms or PBS, 5 days a week, for 6 weeks. End-point analysis was performed 72 h after the last administration of HDM. **B**. The number of total BALF inflammatory cells and inflammatory cell types (alveolar macrophages (AMφ), eosinophils (Eos), lymphocytes (Lymph) and neutrophils (PMN)) from saline- and HDM-challenged *DNA-PKcs*$^{fl/fl}$*; CD11c-Cre* mice were compared to *DNA-PKcs*$^{fl/fl}$ mice, which served as a control (n = 8 – 15 mice, * P < 0.01, *DNA-PKcs*$^{fl/fl}$*; CD11c-cre* + HDM vs. *DNA-PKcs*$^{fl/fl}$ + HDM, one way ANOVA with Bonferroni multiple comparison test). **C**. Representative histologic lung sections stained with hematoxylin and eosin (H&E) or periodic acid-Schiff (PAS) are shown. Scale bars denote 100 µm for the x200 images and 20 µm for the x1000 images. **D**. Quantification of mucous cell metaplasia. (n = 9 mice, *P < 0.0001, *DNA-PKcs*$^{fl/fl}$*; CD11c-cre* + HDM vs. *DNA-PKcs*$^{fl/fl}$ + HDM, unpaired *t* test). 55 + 3.8 airways were analyzed per mouse. **E**. Cytokine secretion by *ex vivo* cultures of mediastinal lymph node cells that had been re-stimulated with saline or HDM (100 µg/ml) (n = 7 – 13 mice, *P < 0.001 *DNA-PKcs*$^{fl/fl}$*; CD11c-cre* + HDM vs. *DNA-PKcs*$^{fl/fl}$ + HDM, one way ANOVA with Bonferroni multiple comparison test). **F**. BALF chemokines. (n = 8 – 12 mice, *P < 0.01, *CD11c-cre* + HDM vs. *DNA-PKcs*$^{fl/fl}$ + HDM, one way ANOVA with

Bonferroni multiple comparison test). **G**. Serum HDM-specific IgE. (n = 8 – 16 mice, *P < 0.0001, *CD11c-cre* + HDM vs. *DNA-PKcs*$^{fl/fl}$ + HDM, one way ANOVA with Bonferroni multiple comparison test). Results are pooled data from two independent experiments.

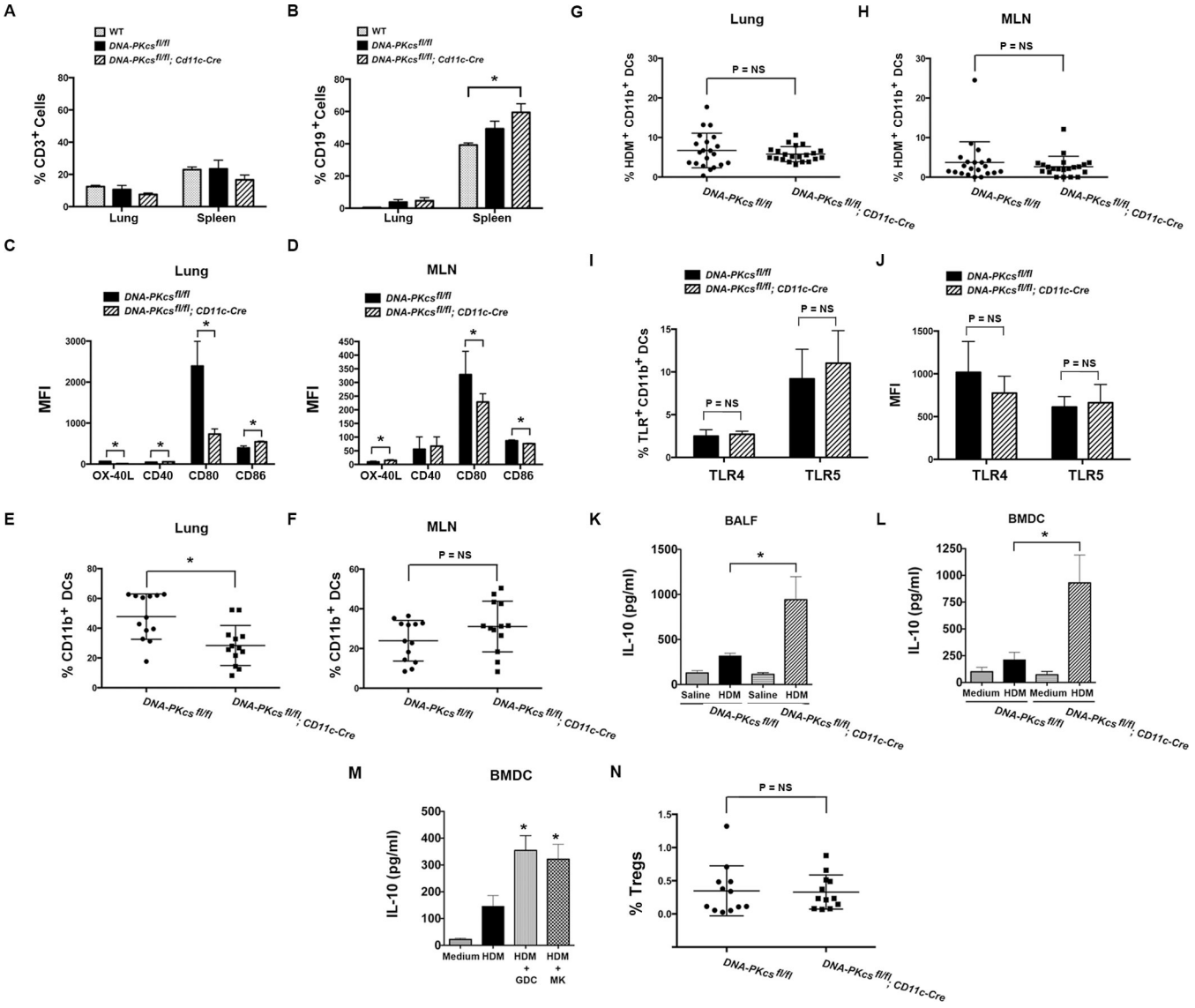

Figure 6. Characterization of HDM-challenged CD11c-specific *DNA-PKcs* Knockout Mice

A & B. The percentage of $CD3^+$ T cells (A) and $CD19^+$ B cells (B) in lungs and spleens of naïve, wild type (WT) C57BL/6 mice, which is the parental strain of both *DNA-PKcs*$^{fl/fl}$ mice and *DNA-PKcs*$^{fl/fl}$*; CD11c-Cre* mice (n = 6, *P < 0.05, one-way ANOVA with Sidak's multiple comparison test). Pooled data from two independent experiments. **C & D**. Mean fluorescence intensity (MFI) of OX-40L, CD40, CD80 and CD86 expression by $CD11c^+$/$MHCII^{hi}$/SSC^{lo} DCs in lungs (C) and mediastinal lymph nodes (MLN) (D) of HDM-challenged *DNA-PKcs*$^{fl/fl}$ mice and *DNA-PKcs*$^{fl/fl}$*; CD11c-Cre* mice (n = 5 – 6 mice, * P < 0.05, Mann Whitney test). **E & F**. The percentage of $CD11c^+$/$MHCII^{hi}$/SSC^{lo} DCs that express CD11b in the lungs (E) and MLNs (F) of HDM-challenged *DNA-PKcs*$^{fl/fl}$ mice and *DNA-PKcs*$^{fl/fl}$*; CD11c-Cre* mice (n = 13 mice, * P < 0.0025, Mann Whitney test). **G & H**. Uptake of HDM by $CD11c^+$/$MHCII^{hi}$/SSC^{lo}/$CD11b^+$ DCs in the lungs (G) and MLNs (H) of *DNA-PKcs*$^{fl/fl}$ mice and *DNA-PKcs*$^{fl/fl}$*; CD11c-Cre* mice 72 hours after administration of HDM extract (50 μg) labeled with Alexa Fluor® 647 (n = 21 mice, P = NS, unpaired *t* test).

I & J. The percentage of $CD11c^{+}/MHCII^{hi}/SSC^{lo}/CD11b^{+}$ DCs that express TLR4 or TLR5 (I) and the MFI of TLR4 and TLR5 expression (J) by $CD11c^{+}/MHCII^{hi}/SSC^{lo}/CD11b^{+}$ DCs in the lungs of *DNA-PKcs*$^{fl/fl}$ mice and *DNA-PKcs*$^{fl/fl}$*; CD11c-Cre* mice (n = 8 mice, P = NS, Mann-Whitney test). **K**. BALF IL-10 (n = 9, * P < 0.01, *DNA-PKcs*$^{fl/fl}$*; CD11c-Cre* + HDM vs. *DNA-PKcs*$^{fl/fl}$ + HDM, one way ANOVA with Bonferroni multiple comparison test). **L**. IL-10 secretion by bone marrow-derived dendritic cells (BMDCs) (n = 7 – 9, * P < 0.01, *DNA-PKcs*$^{fl/fl}$*; CD11c-Cre* + HDM vs. *DNA-PKcs*$^{fl/fl}$ + HDM, one way ANOVA with Bonferroni multiple comparison test). **M**. IL-10 secretion by BMDCs stimulated with HDM (100 ug/ml) with or without Akt inhibitors, GDC0068 (GDC) and MK2206 (MK), both at 1 uM for 24 hrs (n = 8, * P < 0.05, HDM vs. HDM + Akt inhibitor, one way ANOVA with Bonferroni multiple comparison test). Pooled data from two independent experiments. **N**. The percentage of $CD3^{+}/CD4^{+}/CD25^{+}/Foxp3^{+}$ regulatory T cell (Tregs) in MLNs from saline- and HDM-challenged *DNA-PKcs*$^{fl/fl}$*; CD11c*-Cre mice were compared to *DNA-PKcs*$^{fl/fl}$ mice, which served as a control (n = 12 mice, P = NS, Mann Whitney test).

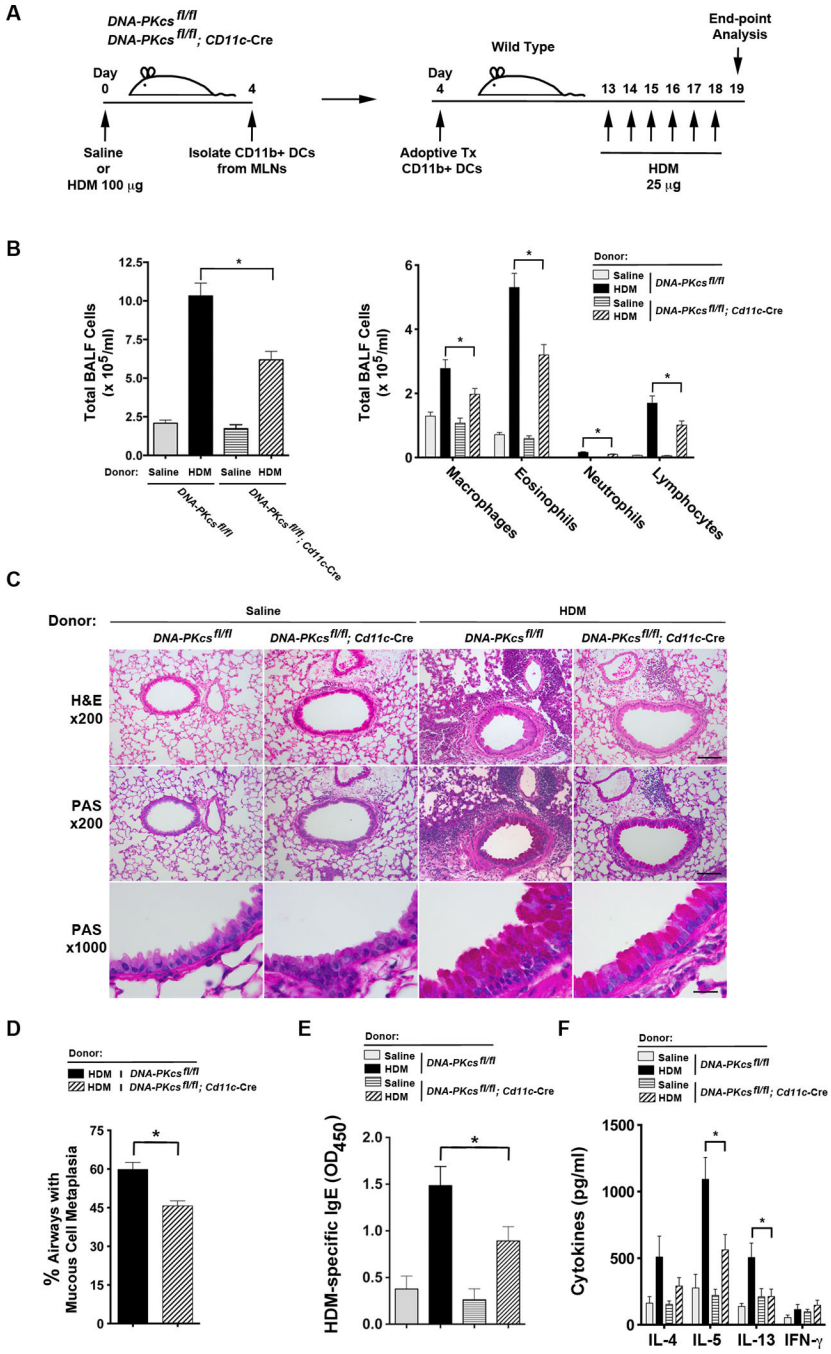

Figure 7. The adoptive transfer of CD11b$^+$ DCs from CD11c-specific*DNA-PKcs*Knockout Mice have an Impaired Ability to Induce HDM-mediated Airway Inflammation

A. *DNA-PKcs$^{fl/fl}$* and *DNA-PKcs$^{fl/fl}$; CD11c-Cre* donor mice received a single intranasal dose of 100 μg of HDM extract or saline and after 4 days, mediastinal lymph nodes were removed and CD11c$^+$/CD11b$^+$/SiglecF$^-$/MHCII$^+$ DCs were isolated by flow cytometry. 2.5 × 10^4 CD11c$^+$/CD11b$^+$/SiglecF$^-$/MHCII$^+$ DCs were adoptively transferred to wild type C57BL6 recipient mice by intranasal administration on day 4 and daily intranasal HDM challenges (25 μg) were administered on days 13 through 18 to all recipient mice. Mice were

sacrificed for end-point analysis on day 19. **B**. The number of total BALF inflammatory cells and inflammatory cell subtypes in recipients of adoptively transferred $CD11b^+$ DCs (n = 6 – 10, * $P < 0.05$, one way ANOVA with Bonferroni multiple comparison test). **C**. Representative histologic lung sections stained with hematoxylin and eosin (H&E) and periodic acid-Schiff (PAS). Scale bars denote 100 μm for the x200 images and 20 μm for the x1000 images. **D**. Quantification of mucous cell metaplasia. (n = 10, * $P = 0.0005$, unpaired *t* test). 48.7 + 3.3 airways were analyzed per mouse. **E**. Serum HDM-specific IgE (n = 6 – 10 mice, * $P < 0.05$, one way ANOVA with Bonferroni multiple comparison test). **F**. Cytokine secretion by *ex vivo* cultures of mediastinal lymph node cells that had been re-stimulated with HDM (100 μg/ml) (n = 6 – 8 mice, * $P < 0.01$, one way ANOVA with Bonferroni multiple comparison test). Results are pooled data from two independent experiments.

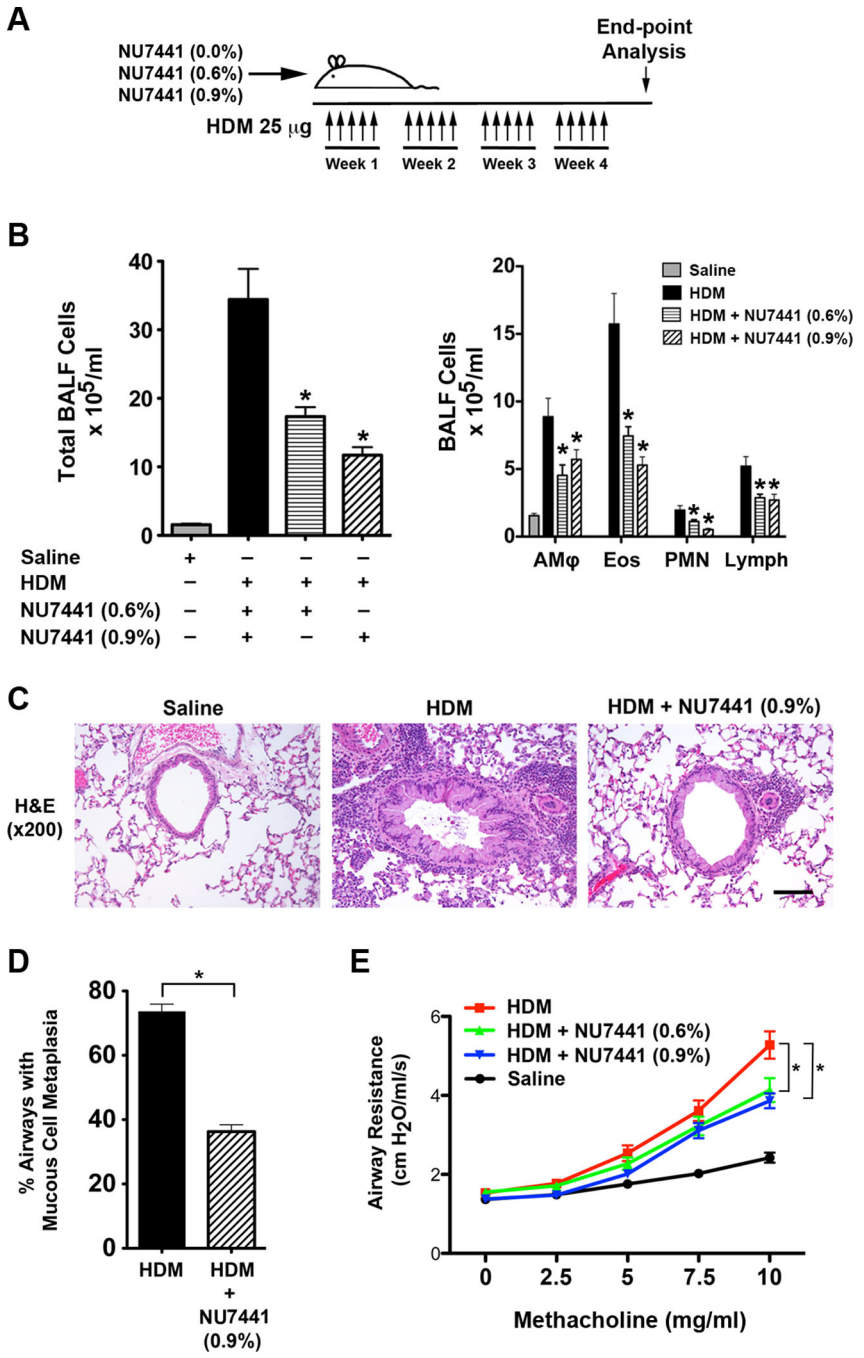

Figure 8. Oral administration of the DNA-PK inhibitor, NU7441, Attenuates HDM-induced Allergic Inflammation, Mucous Cell Metaplasia and Airway Hyperresponsiveness

A. Wild type BALB/c mice were sensitized and challenged by daily intranasal administration of HDM (25 ug) or PBS, five days a week for four weeks. Mice were fed chow that contained 0%, 0.6% or 0.9% NU7441 coincident with the HDM sensitization and challenges. **B**. The number of total BALF inflammatory cells and inflammatory cell types (alveolar macrophages (AMφ), eosinophils (Eos), neutrophils (PMN) and lymphocytes (Lymph)) from saline- and HDM-challenged BALB/c mice that had or had not been fed

chow containing 0.6% or 0.9% NU7441 (n = 20 – 35 mice, * P < 0.05, HDM vs. HDM + NU7441, one way ANOVA with Bonferroni multiple comparison test). **C**. Representative histologic lung sections stained with hematoxylin and eosin (H&E). The scale bar denotes 100 μm. **E**. Quantification of mucous cell metaplasia. (n = 20 mice, *P < 0.0001, HDM + NU7441 vs. HDM alone, unpaired *t* test). 45 + 2 airways were examined per mouse. **D**. Airway resistance (cm H_20/ml/s) to inhaled methacholine. (n = 17 – 20 mice, * P < 0.001, HDM vs. HDM + NU7441, two-way ANOVA with Bonferroni post-test). Results are pooled data from two independent experiments.

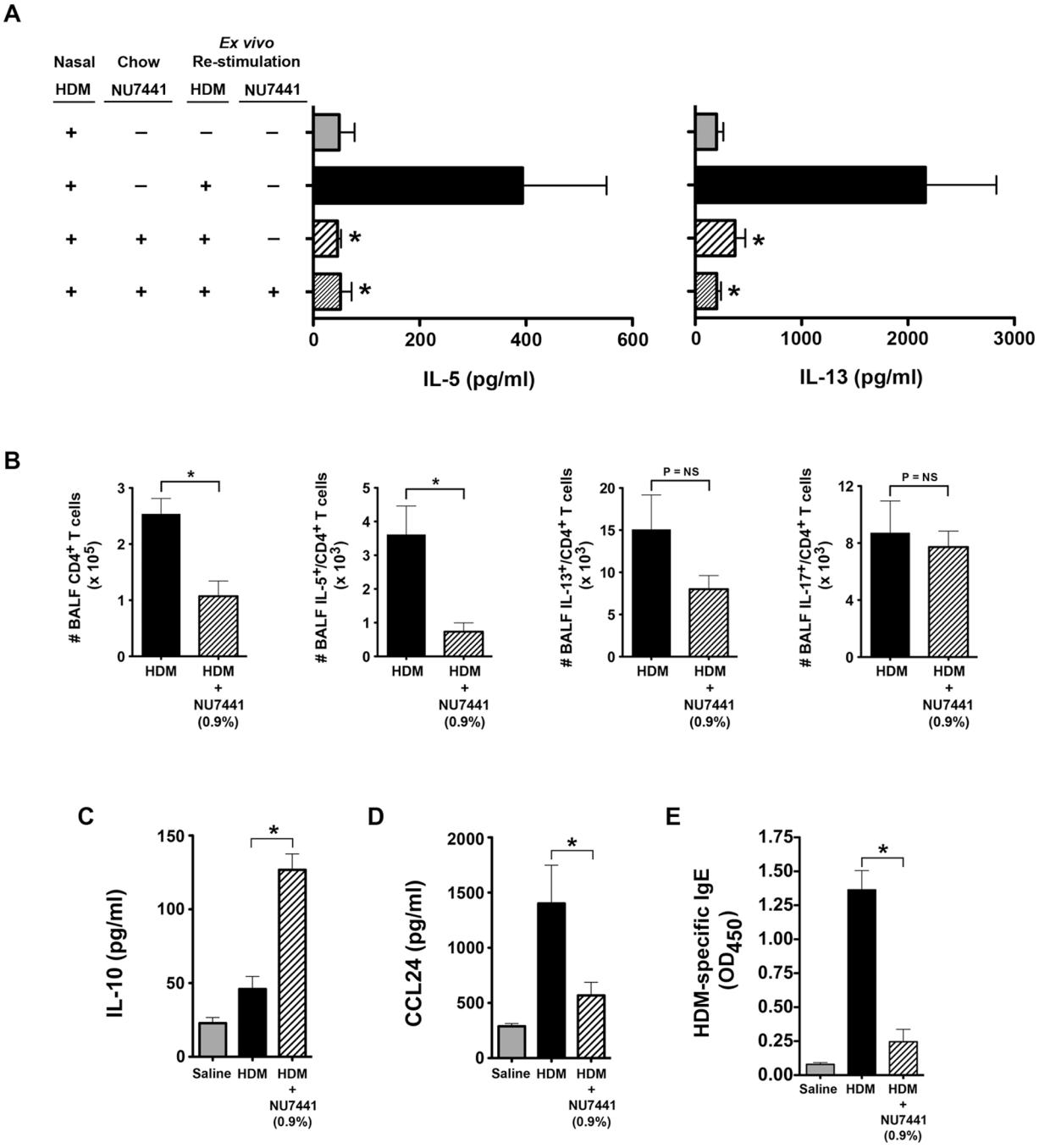

Figure 9. Oral administration of the DNA-PK inhibitor, NU7441, Attenuates HDM-induced Allergic Inflammation and IgE production

A. Th2 cytokine production by mediastinal lymph node cells from HDM-challenged mice that had or had not been fed chow containing 0.9% NU7441 and re-stimulated *ex vivo* with or without HDM (100 μg/ml) and NU7441 (0.5 uM) (n = 6 – 12 mice, * $P < 0.05$, vs. HDM, one way ANOVA with Bonferroni multiple comparison test). **B**. The total number of $CD4^+$ T cells, as well as $IL\text{-}5^+/CD4^+$ and $IL\text{-}13^+/CD4^+$ T cells in bronchoalveolar lavage fluid (BALF), was quantified by flow cytometry (n = 10 mice, * $P < 0.01$, Mann Whitney test). **C**.

BALF IL-10 (n = 7 – 12 mice, * P < 0.001, one way ANOVA with Bonferroni multiple comparison test). **D**. BALF CCL24 (n = 19 – 36 mice, * P < 0.01, one way ANOVA with Bonferroni multiple comparison test). **E**. Serum HDM-specific IgE. (n = 16 mice, * P < 0.001, one way ANOVA with Bonferroni multiple comparison test). Results are pooled data from at least two independent experiments.

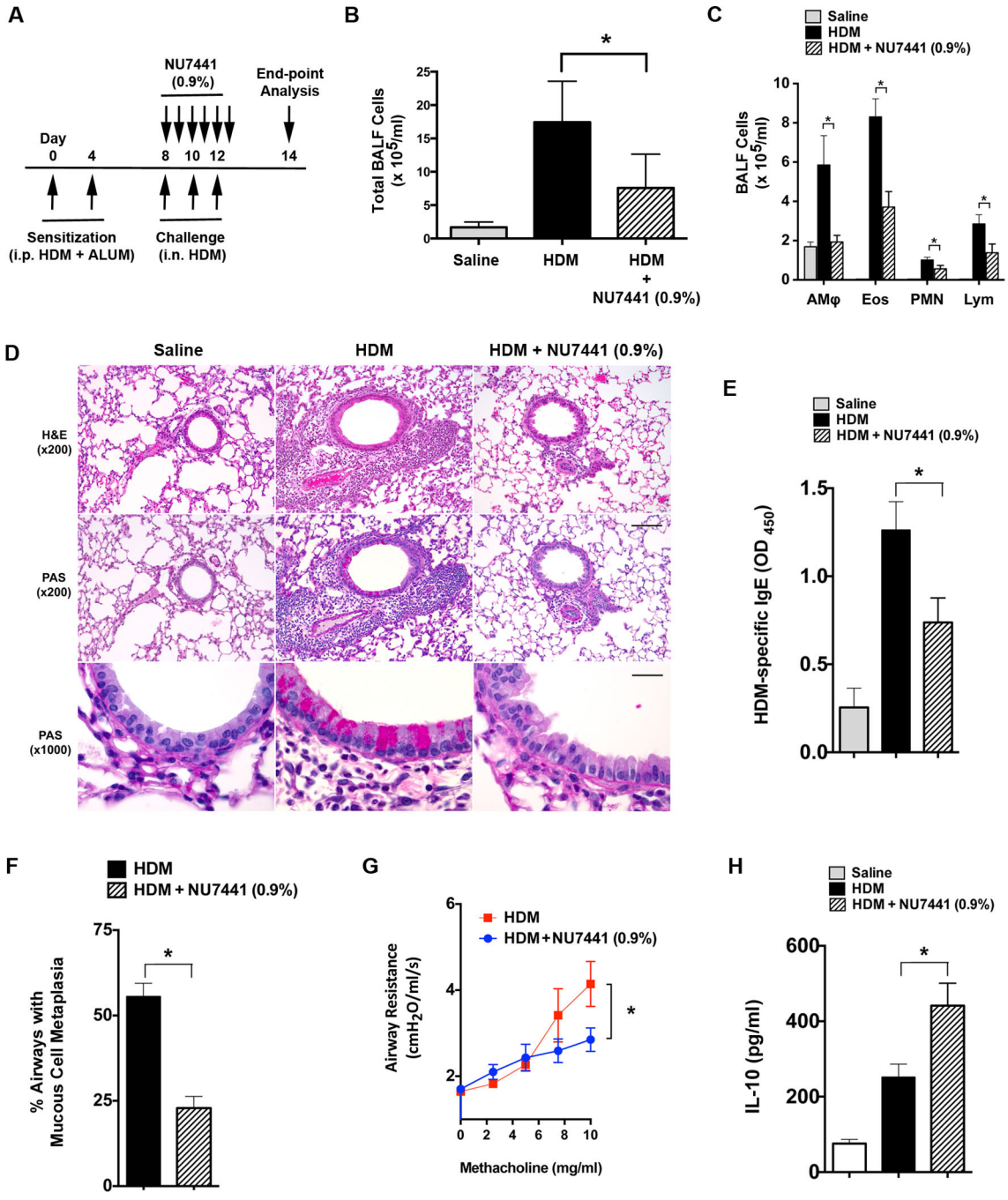

Figure 10. Oral administration of the DNA-PK inhibitor, NU7441, During the Challenge Phase Attenuates the Manifestations of Experimental HDM-induced Asthma

A. Wild type BALB/c mice were sensitized by intraperitoneal administration of HDM (100 μg) and aluminum hydroxide (3 mg) on days 0 and 4. Mice received intranasal challenges with HDM (100 μg) on days 8, 10 and 12 to induce experimental asthma and were concurrently fed chow that contained NU7441 (0.9%) on days 8 through 12. End points were assessed on day 14. **B** and **C**. The number of total BALF inflammatory cells (Panel B) and inflammatory cell types (alveolar macrophages (AMφ), eosinophils (Eos), neutrophils

(PMN) and lymphocytes (Lymph)) (Panel C) were significantly reduced in HDM-challenged WT mice that had been fed chow containing NU7441 (0.9%) during the challenge phase as compared to WT mice that had received regular chow (n = 10 mice, * P < 0.05, HDM vs. HDM + NU7441 (0.9%), one way ANOVA with Sidak's multiple comparison test). **D**. Representative histologic lung sections stained with hematoxylin and eosin (H&E). Scale bars denote 100 μm for the x200 images and 20 μm for the x1000 images. **E**. Serum levels of HDM-specific IgE were quantified by ELISA. (n = 10 mice, * P < 0.05, HDM vs. HDM + NU7441 (0.9%), one way ANOVA with Sidak's multiple comparison test). **F**. Quantification of mucous cell metaplasia. (n = 10 mice, *P < 0.0001, HDM vs. HDM + NU7441 (0.9%), unpaired *t* test). 58.4 + 2.8 airways were examined per mouse. **G**. Airway resistance (cm H_20/ml/s) to inhaled methacholine (10 mg/ml) was significantly reduced in mice that were fed chow that contained NU7441 (0.9%). (n = 10 mice, * P =, HDM vs. HDM + NU7441, unpaired *t* test). **H**. BALF IL-10 (n = 10 mice, * P < 0.01, HDM vs. HDM + NU7441 (0.9%), one way ANOVA with Sidak's multiple comparison test).